UCLouvain

École polytechnique de Louvain

Study of the Western Europe energy transition: an EROI-based analysis resorting on typical days

Author: **Oscar DE GIEY**
Supervisors: **Hervé JEANMART, Gauthier LIMPENS**
Readers: **Emmanuel DE JAEGER, Gian-Marco RIGNANESE, Elise DUPONT**
Academic year 2018–2019
Master [120] in Mechanical Engineering

Abstract

As industrialized countries begin to apprehend the energetic transition, high efforts are being poured in the development of a self-sustainable, efficient and carbon-free society. In order to fulfil this transition, renewables must become the major energy production system of our society. As this noble objective is globally shared, this abrupt transition is not without consequences and challenges. Because of the inherently intermittent energy production, renewables have to be coupled with optimized energy storage. The implementation of these challenging future energy systems has to be modelled beforehand. This study uses an Energy Return On Investment (EROI) optimizing model developed at UCLouvain in 2018 to simulate the energetic transition of North West Europe based on a scenario developed by the European Commission. In order to do so, the existing model has been enhanced with the "typical days" method, allowing for a lower computation time without affecting the results. Thanks to this new model, this study was able to highlight three notable results. During the energetic transition, a correlation was shown between the gas & coal share and the total export of one's country. The total emissions of North West Europe should decrease within the European Commissions plan, but not within the boundaries proposed by the European Union. Finally, the EROI has been shown to decrease with an increasing share of renewables thus questioning the energetic relevance of high shares of renewables in North West Europe.

Acknowledgements

First of all, I would like to thank Professor Hervé Jeanmart for making this topic and master thesis possible, fostering thus the research around energy system's modelling as each year through the propositions of countless extremely interesting master thesis to his students.

As second readers, I would like to thank Professor Emmanuel De Jaeger, Professor Gian-Marco Rignanese and Elise Dupont.

My deepest gratitude goes to Gauthier Limpens for his infinite patience, his high availability and the countless explanations concerning energy systems, linear programming and of course, the subtleties of the "typical days".

As a complete beginner in Python at the beginning of this master thesis, a special thanks goes to Adrien Couplet who helped me out more than once when I had programming hurdles. The access that he granted me to his home-made 8-core server, gave a nice push to the processing capabilities of this master thesis.

I must express my gratitude to the two complete readers of this master thesis: Salomé Van Bunnen who had the courage to read unintelligible pages of mathematics and Gregoire Chapelle who kindly corrected the English and structure mistakes as an energy engineer.

Thank you to my family who supported me through these 5 years at the EPL.

A last acknowledgment goes to my 5 year old computer who suffered tremendously during the last months through multiple night-long simulations and countless graphics renderings and to whom I am grateful for not letting me down in the middle of a simulation.

Contents

Abbreviations

CCGT	combined cycle gas turbine
CO2	carbon dioxyde
DoD	depth of discharge
EROI	energy return on energy invested
ESOI	energy stored on energy invested
EU	European Union
GHG	green house gas
LCA	life cycle assesment
LCOE	levelised cost of energy
LDC	load duration curve
LP	linear problem
LT	life time
MES	multi-energy system
NrTD	number of typical days
NWE	North West Europe
PHES	pumped hydroelectric energy storage
PP	power plants
PtG	power-to-gas
PV	photovoltaic
RE	renewable energy
ROI	return on investment
TD	typical days
WT	wind turbines

Introduction

As industrialized countries seem to have understood the ecological and societal shift they are enduring, high efforts are being poured into the development of a self-sustainable, efficient and carbon free society. Indeed, in the perspective of the ecological transition, multiple ambitious and legally binding objectives are being set at national levels but also at international summits such as the United Nations Climate Change Conferences. As international cooperation towards such a noble objective is impressive, the pledge of a transition of this extent is not without consequences and challenges. In 2018, 42% of all energy-related carbon dioxyde (CO2) came from the power sector causing it to remain the largest source of energy-related emissions [5]. It is therefore increasingly critical that the power sector must be at the forefront of the ecological transition. In order to do so, renewables are recently preferred in our power systems in terms of international dependency and ecology.

Initial economic concerns around renewables were quickly discarded whereas structural issues appeared to be challenging. Indeed, the renewable energy (RE)'s produce electricity in an intermittent, non predictable way whereas electricity demand fluctuates around a mean constant value. Because of this incompatibility, efficient mid and long term storage could be the answer. However, this solution requires long term planning and careful research before launching the necessary investments.

Fostering the research around energy systems and creating a real expertise in this domain will thus lead to the possibility of implementing the wanted electrical transition. Since this expertise is becoming essential, thoroughly understanding our modern power systems and being capable of modelling them accurately in energy models is of paramount importance. Unfortunately, in these models, high time resolution of production systems coupled with up to seasonal storage increases drastically the complexity of these simulations. The challenge is thus to produce power system models coupling high time resolution results with a low complexity of problem.

In the literature, a large choice of energy models can be found and the extensive work of regrouping these models as well as their characteristics, such as their programming language, can be found in [31]. For example, we have: renpass (as a power system simulation model for Germany and neighbouring countries) [9] and OSeMOSYS (an energy system model framework) [27]. The model that will be used in this study is programmed in Python and can simulate the power system of North West Europe (NWE) such as described in [34]. This model has been chosen for several reasons; it was the continuity of undergoing research at the UCLouvain, it has a new optimized approach, it is open source and it already has the large scope of NWE. Indeed, this optimization model optimizes an unusual parameter: the energy return on energy invested (EROI), in opposition to numerous studies optimizing the levelised cost of energy (LCOE) or the return on investment (ROI) metric as objective function [7, 19, 16, 36]. The EROI, which is defined as the *ratio between the useful energy delivered and the total energy invested*, is used as metric. As Python is used in this model, it allows for a more widespread use as it is available in open source on Github. [1].

As this model delivers interesting results, the year-long simulation on an increasingly complex system becomes very time-consuming and impossible to realize without a high processing power. Increasing the complexity for larger results seems thus impossible without drastically simplifying the simulated problem and keeping similar results. As this program runs a linear problem (LP) resolution, reducing the redundant variables would thus proportionally reduce the complexity of the problem. This can be obtained with the method of typical days (TD). This method considers that multiple days in the year may be similar to each other. Hence, it is not necessary to modelize all of them. The TD method can be found in [30] and can be seen implemented in an energy system in [24]. The correct implementation of this method inside the EROI model would pave the way to a simpler, faster and most efficient simulation of our increasingly complex energy systems.

In light of the above, two clear objectives to be fulfilled by the end of the master's thesis can be set:

1. Implement and verify the consistency of the new model resorting to TD
    - Modification of the program to integrate TD
    - Verification of the new model and assessment of the performances
2. Conduct new studies on NWE case scenarios :
    - Analyze the European Commission scenario for 2030
    - Analyze the evolution of the renewables share of NWE

This document will be articulated as follows. The Chapter 1 contextualizes briefly the main ideas of the EROI model; the description of the scope and the implementation. Some minor changes brought to the program will also be discussed. It is to be noted that this chapter will be very similar with regard to content with the master thesis of Adrien Couplet as we both use the same program as starting point. Chapter 2 will extensively discuss the different changes operated, compared to [34], through three different explanation steps: the general concept, the method used and the exact implementation in the model. Chapter 3 will validate the two sides of the implementation: finding appropriate typical days and implementing them correctly into the model. Chapter 4 will finally address a new case scenario to analyze with the newly implemented program using typical days and conduct different studies on the sensitivity of interconnection and the impact of an increasing share of renewables.

[1] `https://github.com/sramelot/memoire2018`

Chapter 1

Context

The model developed in this work is directly linked to the tremendous work done by T. Martinelle and S. Ramelot in their master thesis: "Study of a 100% Renewable Electricity System for Western Europe: an EROI-based analysis" [34]. This work itself is highly inspired by G. Limpens and H. Jeanmart in their article: "Electricity storage needs for the energy transition : an EROI based analysis illustrated for the case of Belgium" [23]. This chapter will focus on the main ideas of the previous modelizations in order to fully apprehend the modifications that were implemented. Two specific objectives will consequently be laid out for this work.

1.1 EROI model

The purpose of the research of [34] was to extend the model [23]. Indeed, the first work's purpose, hereafter refered as "*EROI Belgium*", was to assess the storage needs of Belgium for its energetic transition. This optimization model was based on optimizing RE assets and storage by maximizing the EROI while respecting power flux constraints. The new work, later refered as "EROI Europe", extended the EROI Belgium model to NWE. In order to do so, the hourly-based model developed in EROI Europe was first translated from MATLAB to the open-source language Python and then extended to NWE. The new model, EROI Europe, takes new energy production sources into account and provides a variable number of cells representing different NWE countries.

1.1.1 Description

The EROI Europe model studies the electricity system of a given area for a given period and time step. In this model, the area is divided in "*cells*" and the complete electricity system gathering all cells and their interconnections is refered to as the "*system*". A cell is represented by producers, storage systems, transmission lines, pipelines and a consumption profile. A graphical representation of a cell is given in Figure 1.1a and of a three-cell system in Figure 1.1b.

Four different renewable electricity production systems are considered in this model:

- *Photovoltaic panels*, characterized by the technical parameters of a photovoltaic (PV) panel (efficiency, lifetime and energy cost), irradiance data, an average load factor, an already-installed capacity and a technical potential.

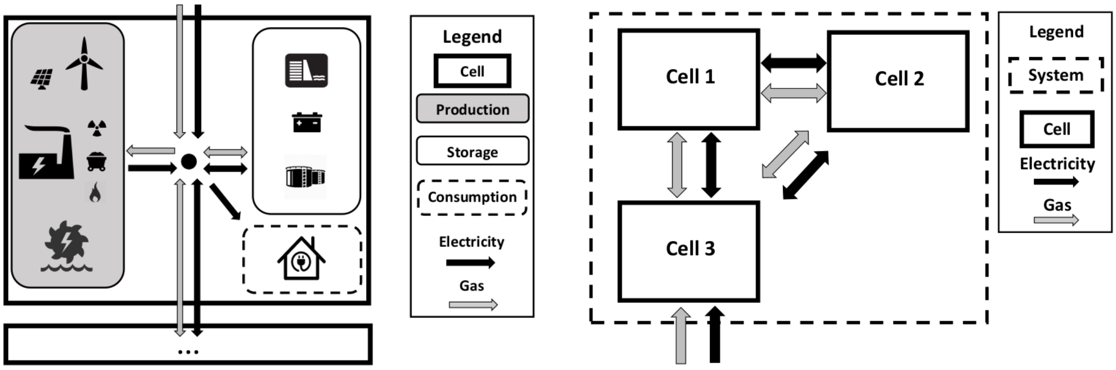

(a) Representation of a cell *(b) Representation of a system*

Figure 1.1: *Representation of a cell and a system, from [23]*

- *Wind turbines*, characterized by a wind turbines (WT) model (cut-in, cut-off and rated wind speed, rated power, lifetime and energy cost), wind speed data, an average load factor, an already-installed capacity and a technical potential.
- *Dams*, characterized by local inflow data, installed storage and output power capacities.
- *Run-of-the-river power stations*, characterized by local inflow data and installed capacity (no storage capacity).

Three different non-renewable (conventional) electricity production systems are considered in this model: *combined cycle gas turbine (CCGT), power plants (PP)*, *Coal PP* and *Nuclear PP*. All three electricity production systems are identified by their total installed capacity and the fuel-to-electricity efficiency. In this model, both CCGT and coal electricity production is assumed to vary instantaneously while the production from nuclear power plants is assumed to be non-flexible, acting as base-load.

In order to store the electricity, three storage systems are considered: batteries, pumped hydroelectric energy storage (PHES) and power-to-gas (PtG). Storage systems are defined by a storage capacity, a charge and discharge rate, an input and output efficiency, a depth of discharge and a leak. In addition, batteries are characterized by the cost of the batteries, their maximum number of cycles, the already-installed capacity and a technical potential. The power-to-gas and the gas storage are defined by an energy cost and lifetime. PHES is characterized by its energy stored on energy invested (ESOI).

These parameters on the storage systems allows for the implementation of their scale of use in our model: seasonal PtG, mid-term PHES and short term batteries. The normalized stored energy is illustrated in Figure 1.2 for one week of storage with our model in Italy. Indeed, we can see little variation of PtG which is making one complete charge/discharge cycle over the year whereas PHES operates a complete cycle in one week and the batteries in half a day.

One can observe in this figure multiple parameters. The depth of discharge (DoD) is fixed at 80 % for the batteries and charge and discharge rate at 20 %. This is shown in day 312 for example where batteries execute a complete charge - discharge operation in 8 hours and begin and stop always at 20 % of available

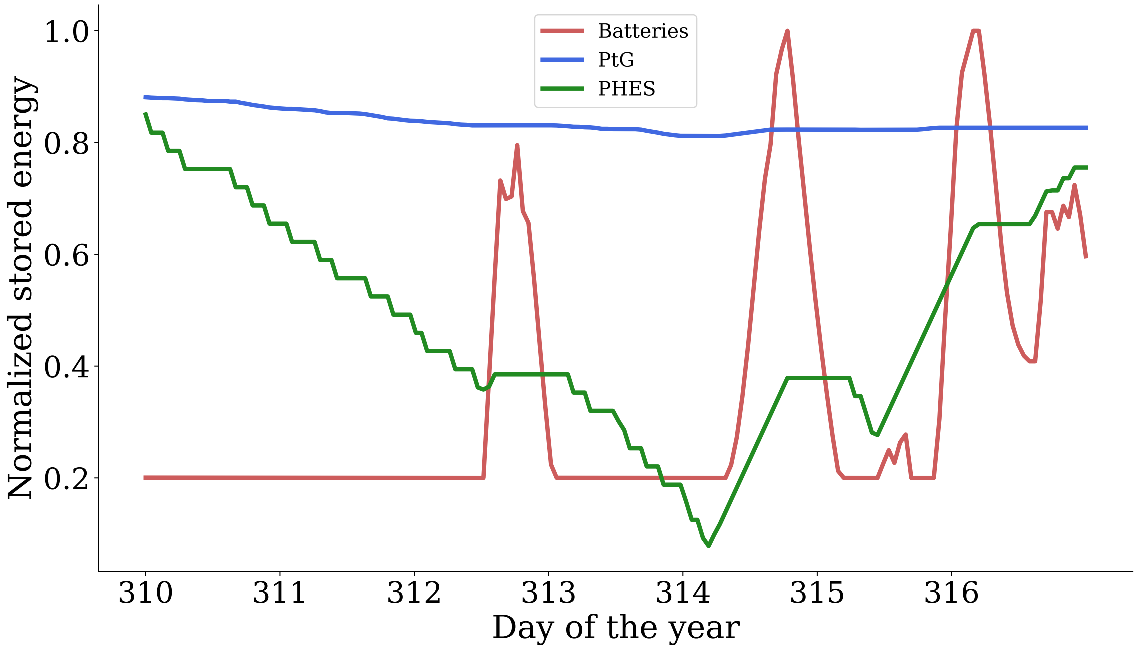

Figure 1.2: *Evolution of the stored energy through the different storage systems over one week in Italy*

stored energy. Because of their respective storage efficiency (highest for batteries and lowest for PtG) the storing priority will always be batteries first, PHES second and PtG last as seen in days 315 and 316.

Consequently, exchanges between countries and imports from outside the system of electricity and gas are possible through transmission lines and pipelines. These exchanges are supposed to be exempt of losses and are identified by a maximum exchange capacity. Imports are characterized by a maximum percentage of the total consumption (at the cell or at the system level).

1.1.2 Objective function and constraints

The EROI of the previously described model is maximized using linear programming. Thus, the objective function of the model must be linear and subject to linear equality and inequality constraints.

Objective function In this model, the net EROI is maximized, which corresponds to the ratio between the end-user consumption from renewable and the energy invested in renewable and storage assets. End-user consumption from renewable is fixed while the energy invested is minimized. The energy invested is defined as the sum of the following components:

1. Energy invested in PV panels and WT.

2. Energy invested in the installation of battery parks, PtG plants and gas storage facilities.

3. Energy invested in the utilization of battery park, PtG plants and PHES.

In the case of batteries and PtG units, the energy investment is split between installation and utilization by the means of a weighting factor to avoid unrealistic behaviours such as a huge park of batteries only used once.

Constraints The linear programming problem is subject to some constraints. The most important constraint is the power balance at every time step and in every cell. Indeed, inside every cell, the production and import of electricity needs to be at least equal to the consumption and export of electricity combined. Then, a minimum RE share of the total electricity production has to be respected in every cell and in the whole system. Similarly, a maximum electricity and gas import share of the total electricity consumption are defined by the user at the cell and system level.

Furthermore, a storage balance is imposed for batteries, PHES, dams and gas storage facilities. Indeed, the energy contained inside a storage system at time t needs to match the energy stored and the energy transfers to or from the storage system at time $t-1$. In addition to this constraint, a minimal use of PtG is imposed in every cell. This minimum utilization constraint defines a minimum ratio between the energy which goes through the PtG unit and the maximum energy that could be absorbed at full load. These constraints are thoroughly explored in Section 2.3.2.

Finally, the system and the cells are constrained by technical limits: the transmission capacity for both electricity and gas between cells is limited and each technology is limited by its minimal installed capacity for RE and its maximal potential.

The full mathematical description of the objective function and the constraints is available in [34].

1.2 North West Europe implementation

By combining the 6 implemented cells of our system, the model is able to optimize the EROI in NWE. A trade-off between computation time and problem accuracy led to the creation of 6 cells, presented in Figure 1.3 and inspired by other works [34][2] :

- Scandinavia: Denmark, Norway and Sweden.
- British Isles: Ireland and the United Kingdom.
- Germany & Benelux: Germany, Belgium, Luxembourg and Netherlands.
- France.
- Italy & Alpine States: Italy, Austria and Switzerland.
- Iberian Peninsula: Portugal and Spain.

These cells tend to recreate similar orders of magnitude in decision factors: population, geographic position, electricity consumption and energetic mix. Even if regions of a same country have completely different decision factors, the decision was made to regroup them because of the national political influence. Indeed, political decisions such as the German nuclear phase-out impacts heavily the energetic mix of the whole country. This model is convenient in terms of data collection and system comprehension but lacks precision due to the electricity transmission

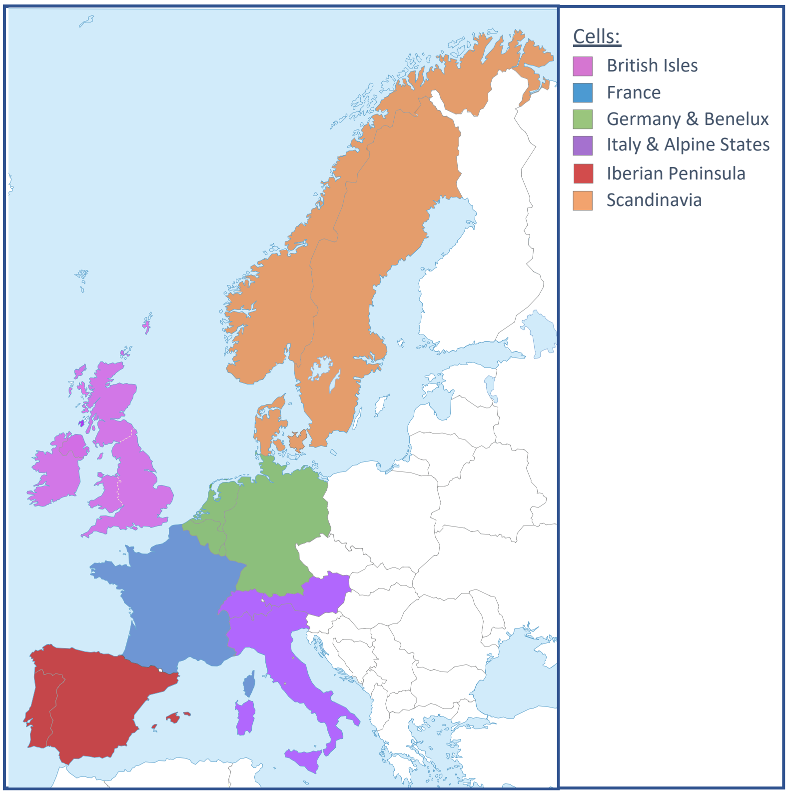

Figure 1.3: *North West Europe cells composition*

between cells and the copper plate hypothesis. This hypothesis could be questioned with countries like Germany developing recurrent congestion between the electricity producing North and the industrial South regions of the country.
Extensive description of the NWE model and its different cells can be found in the EROI Europe model [34].

1.3 Programming implementation

The model is implemented using the Python programming language. The PuLP library is used to write and solve the linear programming problem. PuLP has the ability to interface with multiple solvers such as COIN CBC or CPLEX. This study will use the CPLEX solver from IBM available on the IBM website [1].

Code adjustments It is to be noted that several adjustments have been conducted before the implementation of the TD method with the help of Adrien Couplet. Two errors have been corrected, three improvements implemented and the architecture of the model has been completely redesigned without affecting the results. The complete changes can be found in A.1. A brief explanation about the use of the program's new architecture is presented in A.2. The complete code can be found hosted by Github[2].

[1] `https://www.ibm.com/analytics/cplex-optimizer`
[2] `https://github.com/oscardegiey/EROI-OMES`

Chapter 2

Methodology

The first objective of this work is to implement the new solving method: **the concept of typical days** in the EROI Europe model. We will follow three straightforward steps: understanding *the concept* (Section 2.1), identify an appropriate *method* (Section 2.2) and thoroughly complete *the implementation* (Section 2.3).

2.1 The concept: typical days

Previous work on the EROI optimization generated time issues. Indeed, the optimization problem used hourly resolution in the time frame of a year-long horizon. With respect to the number of variables, the complexity of the problem increases drastically, and so does the computation time. This optimization problem can be sped-up by the introduction of TD. As the RE are organically growing in the multi-energy system (MES), so does their dependency on meteorological factors such as wind, irradiance and hydraulic inflow. Meteorology, as a chaos-governed system [35], is hard to predict accurately and varies greatly with a slight variation in input. However, this study is not concerned by stochastic analysis. Therefore, using instead a non-predictable approach, we can deal with acceptable errors in a defined range. This is achieved by statistically regrouping certain types of days of the year that are very similar to one another. Indeed, recomputing every day of the year when a lot of days resemble each other, would be redundant.

Thus, instead of considering each day of the year independently, a TD will be coupled to a larger set of different days of the year using a clustering method. This set will be called σ(y), defined for every day y such as:

$$y \in 1 \leq y \leq 365,$$

where y is coupled to a corresponding TD thanks to σ

$$\sigma(y) \in 1 \leq \sigma(y) \leq k$$

k being the number of clusters chosen to represent the problem. This technique should not interfere drastically with the results and should significantly reduce the computation time. This methodology and afore-mentioned explanation is inspired by [30] in the Method 1. This method is illustrated in Figure 2.1 where the gray path follows the original study of [34] whereas the red path comprises an intermediate path of clustering reducing the time series and thus the problem.

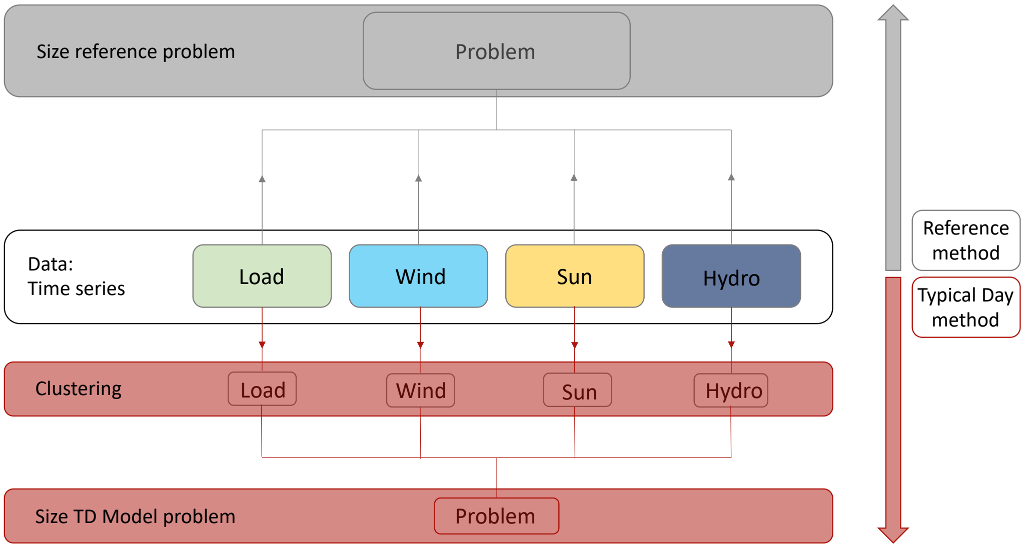

Figure 2.1: *Schematic explaining the methodology difference between the reference model (in gray) and the TD model (in red) to build the linear problem from the data*

2.1.1 Example: British Isles consumption

The example of a TD among other days in the British Isles is used to illustrate the concept of TD in figure 2.2. Indeed, we can observe the typical day used to approximate six other classical days for the input data of power consumption. In this case, using the TD in red instead of 6 different data-sets simplifies greatly any problem taking into account power consumption.

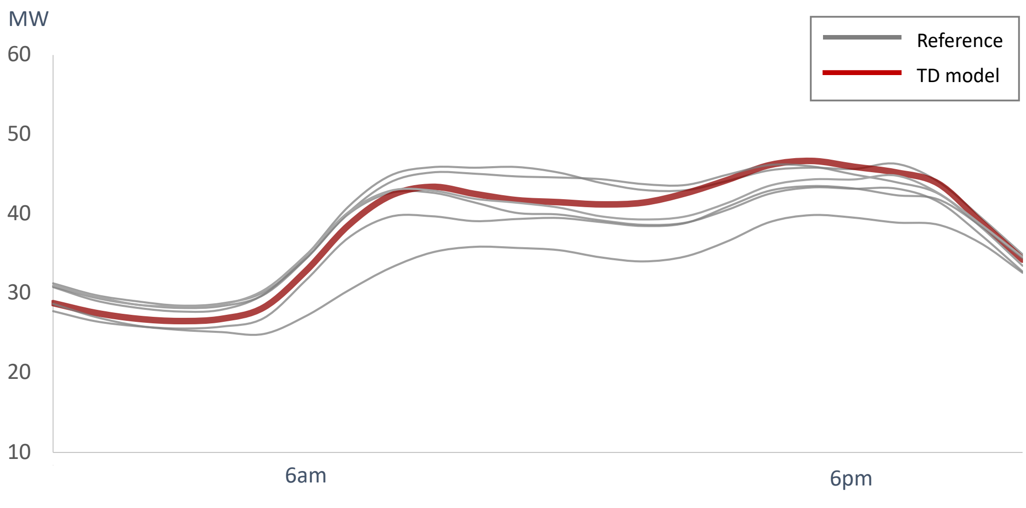

Figure 2.2: *Power consumption of a typical day representing 7 regular days over a day in the British Isles*

This simple application is extended to the entirety of inputs: wind velocity, solar irradiance, local hydraulic inflow and power consumption of the system. These inputs can be weighted in the TD distribution depending on their relative importance to their respective cell. The precise implementation of this concept in the linear problem is detailed in section 2.3.

2.2 The method: k - medoids

Now that the concept of TD is established, the method to find them has yet to be determined. Indeed, a clustering algorithm balancing computation time and precision has to be determined in order to find the optimized set of TD. Multiple clustering methods are used in the literature and the intuitive method of k - medoids was found to yield relatively good performances in multiple studies. [20, 30, 28]

2.2.1 Theory

This algorithm is partitional (meaning it breaks the data set in different sub-groups) and tries to minimize the euclidean distance between a cluster and the point (later referred to as centroid) designed as the center of this cluster. It transforms a data set of n objects in k clusters that are known before the launch of the algorithm. The k - medoids algorithm operates following three steps, inspired by [33] :

1. Initialization of a k subgroup of the n objects as initial medoids
2. Association of each object x to a medoid m following the rule:

$$\underset{m_i \in M}{\text{minimize}}\ dist(x, m_i)^2$$

3. for each medoid m and non medoid x:
   (a) swap m and x, associate each data to the closest medoid and computes the cost following:

$$C_i = \frac{1}{|X_i|} \sum_{x_i \in X_i} |x_i - m_i|$$

   (b) if the computed cost C_i is smaller than the stored cost, store the new cost. If not, undo the step a).

At the end of this converging sequence the algorithm should have reached a local optimum minimizing the squared Euclidean distance (2.1) between the data and their respective cluster.

$$d(x, m) = |x - m|^2 \tag{2.1}$$

2.2.2 Interest and flaws

This method presents some serious advantages: it converges in a fixed amount of iterations to a local optimum and returns a value from the data-set as cluster (ideal for physical models).

Unfortunately, k - medoids comes with some flaws: results can differ from one simulation to another due to different initial clusters and can be very time consuming for large data-sets when a high tolerance is demanded. Indeed the k - medoid method has a high time complexity :$\mathcal{O}(k(n-k)^2)$.

Furthermore, it is a greedy algorithm, hence it will rapidly converge towards a local optimum. It is not intended to find the global optimum, which would require a high computation time to try out all data sets.

The algorithm k - means has the same process but creates a new object for the centroid by computing the mean value, whereas k - medoids uses an existing data as centroid. Since this numerical resolution reflects real-life data, k-medoids has been used for a more relevant approach. Furthermore, using existing data as centroid is less sensitive to noise and outliers and thus less biased compared to the k - means approach [29].

2.2.3 Example: k - medoids with k = 3 clusters

An example with a randomly-generated scatter plot is shown in Figure 2.3 with different steps of the algorithm. For a limited amount of data (such as in the example), we can observe a very rapid convergence of the medoids. Indeed, the local optimal answer is obtained after only ten iterations for three clusters.

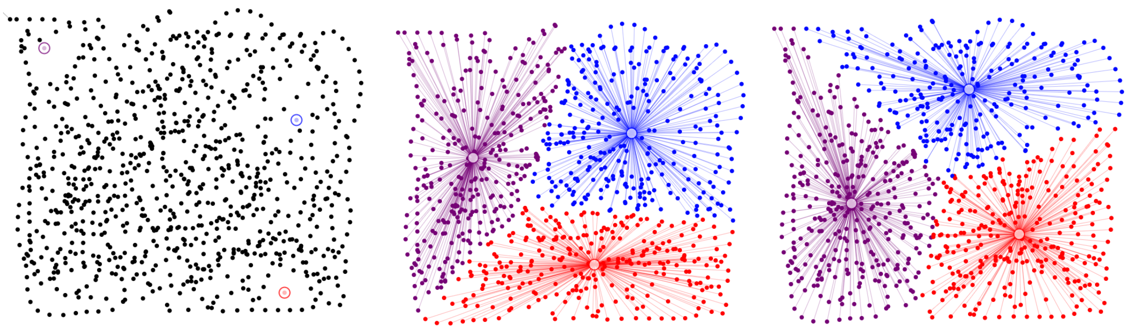

(a) First step: initialization of the medoids. *(b) Second step: second iteration.* *(c) Final clusters after 10 iterations*

Figure 2.3: *Example of three clusters regrouping a randomly generated data set, issued from [37]*

2.3 The implementation

This section will first investigate how to implement the concept of TD in this specific MES and consequently asses the exact implementation of both the clustering method and the TD in the program for the EROI Europe model.

This section will detail the mathematical description of every process. Some variables and parameters undefined until this point can be found at the beginning of this document in the list of symbols. Symbols, subscripts and method of reasoning will be similar to Martinelle's work for the sake of consistency. Every variable will be expressed in function of time t which is part of a time vector discretized by a time step Δt. The variables are thus expressed as an average on the time period $[t; t + \Delta t]$

As the previous model worked on basis of a linear optimization problem, all the changes due to TD method impact the way the problem is built in order to simplify the problem resolution. The implementation follows three different steps in the reasoning behind the construction of our linear problem: description of the objective function, the constraints of our problem and the limits of our variables. Subsequently, an example will illustrate the development.

The information of prime importance to whomever wants to understand and implement TD in a MES is that the *variation* of energy can be simplified, but not the absolute value. Hence, the variation of energy per unit of time is defined as the power. Thus, the modification being allowed by the TD **solely concerns power variables**.

2.3.1 Objective function

As stated in section 1.1.2, the objective function translates the factor the solver has to optimize. In this case, the EROI has to be maximized. The net EROI is defined as the ratio between the energy consumption of the end user and the energy invested to produce it:

$$EROI_{net} = \frac{\text{Energy consumption}}{\text{Energy invested}} \tag{2.2}$$

Please note that in the particular case of RE, their invested energy in the cell c $E^{RE}_{inv,c}$ comprises the investment in the production unit but also the $E^{stor}_{inv,c}$, compensating for the loss of flexibility.

As we receive as input the energy consumption, the objective function of EROI can be translated into minimizing the energy invested (E_{inv}). Once again, the methodology of Martinelle [34] is taken for consistency.

From now, every term in this color in equations/text will be impacted by the TD method.

The energy invested in RE E^{RE}_{inv} takes into account the production, installation, maintenance and dismantling of the RE production unit. Thus, the total E_{inv} for the problem is:

$$E_{\text{inv}} = \sum_{\text{Cell c}} (E^{\text{RE}}_{\text{inv,c}} + E^{\text{stor}}_{\text{inv,c}}) \tag{2.3}$$

The first term of equation 2.3 mirrors the production of PV and WT parks (no energetic cost is associated to dams and run-of-the-river installations) and thus represents an absolute production of energy. The TD method will therefore have no impact on the latter term.

On the other hand, the second term, $E^{stor}_{inv,c}$, comprises different storage units which have different power ratings (for k battery parks):

$$E^{\text{stor}}_{\text{inv,c}} = \sum_{k} E^{\text{bat}}_{\text{inv}} + E^{\text{PtG}}_{\text{inv}} + E^{\text{PHES}}_{\text{inv}} + E^{\text{gas storage}}_{\text{inv}} \tag{2.4}$$

Three of the four energy investments of equation 2.4 are influenced by our implementation. Indeed, the investment for gas storage is an absolute energy value. As explained before, the main change that will be undergone will concern power. Instead of being defined for every hour of every day of the year, power will be linked to the same hour of one of the TD. Thus, the number of power variables will be reduced from $8760/\Delta t$ to number of typical days (NrTD) $*24/\Delta t$. The precise reduction in variables is available at Section 3.3. This process is enforced by linking every time t to an hour of a TD:

$$\mathbf{P^x}(\mathbf{t}) = \mathbf{P^x}(\mathbf{h}, \mathbf{TD}) \tag{2.5}$$

Where $P^x(t)$ is any power used in any computation of energy.

The three remaining terms impacted by the TD method in equation 2.4 are developed hereafter.

Batteries

$$\sum_k E^{\text{bat}}_{\text{inv}} = \sum_k \frac{1}{2}(E^{bat}_{\text{installation,k}} + E^{bat}_{utilisation,k}) \tag{2.6a}$$

The installation of the battery parks is a one time investment linked to capacity and thus not impacted by TD. However, day-to-day utilization is highly dependent of these and its variation is a resultant of this relation:

$$\text{Current model: } E^{bat}_{utilisation,k} = \epsilon^{\text{bat}}_{\text{utilization}} \sum_t (P^{bat}_{in,k}(t)\Delta t) \tag{2.6b}$$

$$\text{Typical days model: } E^{bat}_{utilisation,k} = \epsilon^{\text{bat}}_{\text{utilization,}} \sum_t (P^{bat}_{in,k}(h, TD)\Delta t) \tag{2.6c}$$

Where $\epsilon^{\text{bat}}_{\text{utilization}} = E^{bat}_{cost/Wh}/E^{bat}_{LT/Wh}$, the ratio of the energy cost per Wh to the total enery storable throughout this park's life time (LT).

Power to Gas

$$E^{\text{PtG}}_{\text{inv}} = \frac{1}{2}(E^{PtG}_{\text{installation}} + E^{PtG}_{utilisation}) \tag{2.7a}$$

The installation of the PtG facility is a one time investment linked to capacity and thus not impacted by TD. However, day-to-day utilization is highly dependent of these and its variation is a resultant of this relation:

$$\text{Current model: } E^{PtG}_{utilisation} = \epsilon^{\text{PtG}}_{\text{utilization}} \sum_t (P^{PtG}_{in}(t)\Delta t) \tag{2.7b}$$

$$\text{Typical days model: } E^{PtG}_{utilisation} = \epsilon^{\text{PtG}}_{\text{utilization,}} \sum_t (P^{PtG}_{in}(h, TD)\Delta t) \tag{2.7c}$$

Where $\epsilon^{\text{PtG}}_{\text{utilization,}} = -E^{PtG}_{cost/W}/E^{PtG}_{LT/W}$, the ratio of the energy cost per W installed and the total convertible energy per W.

PHES

$$E_{\text{inv}}^{\text{PHES}} = E_{utilisation}^{PHES} \tag{2.8a}$$

PHES production is based on already installed capacity and thus has no installation costs. The whole term is thus impacted by the TD:

$$\text{Current model: } E_{utilisation}^{PHES} = \epsilon_{\text{utilization}}^{\text{PHES}} \sum_{t} ((P_{in}^{PHES}(t)\Delta t)) \tag{2.8b}$$

$$\text{Typical days model: } E_{utilisation}^{PHES} = \epsilon_{\text{utilization,}}^{\text{PHES}} \sum_{t} (P_{in}^{PHES}(h, TD)\Delta t) \tag{2.8c}$$

Where $\epsilon_{\text{utilization,}}^{\text{PHES}} = (1/ESOI_{PHES})$ is the only cost linked to PHES, expressed as the inverse of the ESOI.

Modified objective function We can thus express the objective function within the scope of our TD method:

$$\begin{aligned} E_{\text{inv}} = \sum_{\text{Cell c}} \Bigg(& E_{\text{inv,c}}^{\text{RE}} + \sum_{k} \frac{1}{2}(E_{\text{installation,k}}^{bat} + \beta(TD) \times E_{utilisation,k}^{bat}(h, TD)) \\ & + \frac{1}{2}(E_{\text{installation}}^{PtG} + \beta(TD) \times E_{utilisation}^{PtG}(h, TD)) \\ & + \beta(TD) \times E_{utilisation}^{PHES}(h, TD) + E_{\text{inv}}^{\text{gas storage}} \Bigg) \end{aligned} \tag{2.9}$$

Where β(TD) is the number of regular days linked to the typical days TD (such as the sum of the vector β is 365). It can be deducted that three major changes have been operated in the objective function and thus in the factor to be optimized: the utilization of the batteries, PtG and PHES.

2.3.2 Constraints

The variables of our problem are limited by certain relationships between them named constraints. This section will detail the constraints impacted by the implementation of our new model of TD. The LP depicts eight different constraints:

1. A minimal RE share in the system production
2. A minimal RE share in the cell production
3. A maximal import in the cell
4. A maximal import in the system
5. **A power balance at each time *t***
6. **A storage balance for each type of storage**
7. **A minimal use of PtG**
8. An equality of power and gas exchanges between every cell

Only three of them are directly impacted by the implementation of TD, we will thus not develop the five others. Their exact implementation in the LP can be found in the section 1.4.2 of [34].

Power balance At every time t and for every cell, the total production should equal the consumption. This is illustrated in Figure 2.4. A greater value of production may happen with RE production, if the energy can't be stored, the excess of energy is then considered as curtailment. The power production comprises every type of production system:

- Gas power plants
- Coal power plants
- Nuclear power plants
- Hydraulic power plants with reservoir (dams)
- Hydraulic power plants without reservoir (runriver)
- PHES, negative if stored and positive if delivered
- Batteries, negative if stored and positive if delivered
- PV farms production
- WT farms production
- Exchange with other cells

To fulfill this constraint, the sum of : the seven power plants and batteries, the PV farms, the WT farms and the exchange with the other cells should be equal or greater than the consumption of the system. Hence :

$$\sum_{m}^{7} P_{PP\&bat}^{m}(t) + P_{PV}(t) + P_{WT}(t) + P_{\text{exchanged}}(t) \geq P_{\text{consumed}}(t) \tag{2.10}$$

Please note that the production of PV and WT is not subject to a direct impact of TD because it's production cannot be optimized; the production is directly linked to natural conditions and not variable. The impact is indirect because the TD model will still optimize the scalar defining the surface of PV and the number of WT's needed to fulfill demand. The TD method thus directly affects the first term of the equation 2.10:

$$\sum_{m}^{7} P_{PP\&bat}^{m}(h, TD) + P_{PV}(h, TD) + P_{WT}(h, TD) + P_{\text{exchanged}}(h, TD) \geq P_{\text{consumed}}(t) \tag{2.11}$$

This power balance is illustrated in Figure 2.4 as an energy balance; it translates the fact that the sum of every production mean (here the storage plus the RE plus the exchange) must be equal to the consumption of the system at all times.

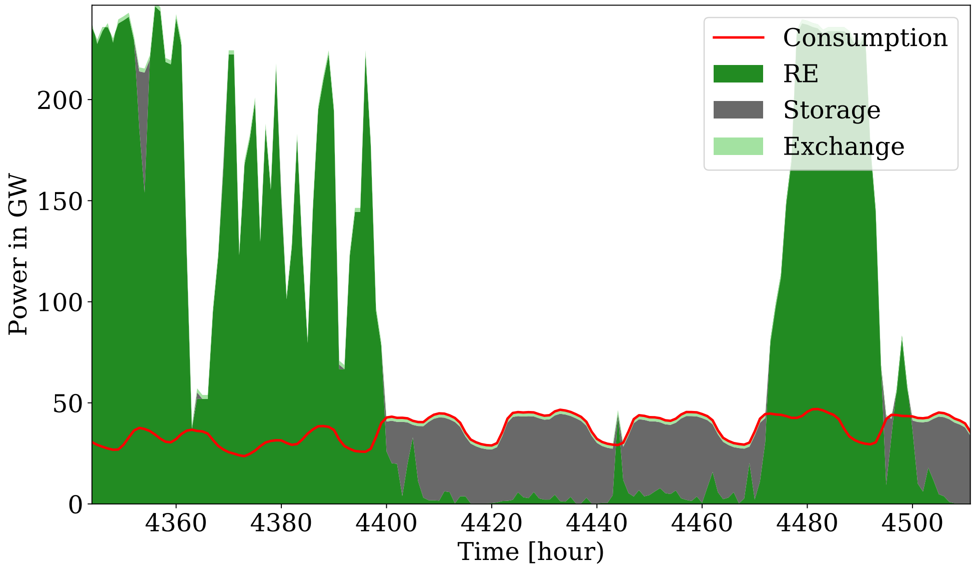

Figure 2.4: *Power balance of a duration of one week for the cell British Isles in a 100 % RE scenario illustrating the power balance constraint*

Storage balance The balance of storage concerns four means of storage: batteries, PHES, dam and gas. It enforces the cyclic conditions of storage; the energy stored at time t - Δt must still be available at time t, and these constraints are required for every cell:

1) For every battery park k in the cell. The energy stored in the batteries of park k at time t is thus equal to the energy stored at t - Δ t times a certain coefficient minus the sum of the energy entering and leaving. The proportionality coefficient $(1-\gamma_k)^{\Delta t}$ represent the leakage of our batteries.

$$E_k^{\text{bat}}(t) = (1-\gamma_k)^{\Delta t} E_k^{\text{bat}}(t-\Delta t) - \left(P_{in,k}^{bat}(t-\Delta t) + P_{out,k}^{bat}(t-\Delta t)\right)\Delta t \tag{2.12a}$$

2) PHES storage constraints mirror the same terms as the battery storage relation apart for the exception og the leakage coefficient which isn't considered.

$$E^{\text{PHES}}(t) = E^{\text{PHES}}(t-\Delta t) - \left(P_{in}^{PHES}(t-\Delta t) + P_{out}^{PHES}(t-\Delta t)\right)\Delta t \tag{2.12b}$$

3) The storage by dam has the particularity of receiving the energy stored by a local water inflow, thus outside of the system. This feed is represented by P_{in}^{dam}.

$$E^{\text{dam}}(t) = E^{\text{dam}}(t-\Delta t) - \left(P_{in}^{dam}(t-\Delta t) + P_{out}^{dam}(t-\Delta t)\right)\Delta t \tag{2.12c}$$

4) The storage using gas as energy vector takes more parameters into account. Indeed, CCGT consumption and exchange in between cells is possible. Thus, the gas available at time t is the sum of gas available at time t - Δt minus what is stored in PtG, used in CCGT and the quantity exported to other cells ($E^{c,c_n}_{\text{gas exch}}$). We finally add to this the imported quantity of gas ($E^{c_n,c}_{\text{gas exch}}$).

$$\begin{aligned} E^{\text{gas}}(t) =& E^{\text{gas}}(t-\Delta t) - \left(P^{PtG}_{in}(t-\Delta t) - P^{CCGT}(t-\Delta t)\right)\Delta t \\ & - \sum_n E^{c,c_n}_{\text{gas exch}}(t-\Delta t) + \sum_n E^{c_n,c}_{\text{gas exch}}(t-\Delta t) \end{aligned} \tag{2.12d}$$

Every single one of these energetic balances (Equations 2.12) must also fulfill a yearly cyclic condition:

$$E^x(0) = E^x(t_{\text{end}}) \tag{2.13}$$

Please note that every power cited is weighted with a respective efficiency (which was not depicted for more clarity). Finally, we can thus observe a global two-term impact of the TD model on equations 2.12. Indeed every character in this color is using the power generated on a specific hour of a specific TD instead of every hour of every day in the year:

$$\mathbf{P^x}(\mathbf{t}) = \mathbf{P^x}(\mathbf{h}, \mathbf{TD}) \tag{2.14}$$

PtG minimal use Because of the uncertainty concerning the further developments and real energetic cost of the PtG technology, a minimum usage has been imposed. This constraint represents a minimum ratio between the gas passing through the PtG facility and the maximum energy that could be absorbed at full load during period T:

$$\text{Current model: } \sum_t P^{PtG}(t) \times \Delta t \geq \alpha P^{PtG}_{max} \times T \tag{2.15}$$

$$\text{TD model: } \sum_t P^{PtG}(h, TD) \times \Delta t \geq \alpha P^{PtG}_{max} \times T \tag{2.16}$$

Where α is a minimal time use.

2.3.3 Variable limits

Variable limits concern particular constraints: variables limited by scalars. The scalars are given as input of the problem and have been chosen as realistic value in the context of our system. Nine types of parameters are limited:

1. Electricity: the electrical exchange between two cells is limited by the capacity of their interconnection (which may differ depending on the direction of the exchange).

2. Gas: Much like electricity, the gas exchange between two cells is limited by the capacity of their interconnected pipelines (which may also differ direction-wise).

3. Non-RE: the production of coal, nuclear and CCGT PP are strictly limited to their installed capacity as upper limit.

4. PV and WT: the production is limited by a lower limit to their pre-installed capacity. The upper limit is defined as a potential expressed in numbers and in area of panels for respectively WT and PV farms.

5. Dam and PHES: the hydraulic production is constrained by three limits. The energetic content of our hydraulic PP is limited by the capacity of its reservoir. The power entering the reservoir is bound to the local inflow and the power generation has an upper limit of installed capacity. In the case of PHES, pumped power is bound to the installed capacity.

6. Run-of-the-river: the production is very similar to a dam only without the ability to store the energy in a reservoir. An upper limit of installed capacity is defined for power generation

7. **Batteries**: batteries storage is optimized and has an upper and a lower capacity limit given as input, weighted by charging and discharging rates. The DoD is taken into account by imposing that a battery cannot be entirely discharged.

8. **PtG**: the storage through PtG is optimized and has a set upper and a lower capacity.

9. Gas storage: The optimized content of the gas reservoir should also lie between the lower filling limit and its capacity.

Comprising direct power utilization, batteries are indeed affected by the model shift:

$$E^{bat}_{\mathrm{min,k}} \leq E^{\mathrm{bat}}_{\mathrm{opt,k}} \leq E^{\mathrm{bat}}_{\mathrm{max,k}} \tag{2.17a}$$

$$\forall t : -E^{\mathrm{bat}}_{\mathrm{opt,k}}\alpha_{\mathrm{k}} \leq P^{bat}_{in,k}(t) \leq 0 \tag{2.17b}$$

$$\forall t : 0 \leq P^{bat}_{out}(t) \leq E^{\mathrm{bat}}_{\mathrm{opt,k}}\alpha_{\mathrm{out}} \tag{2.17c}$$

$$\forall t : E^{\mathrm{bat}}_{\mathrm{opt,k}}(1 - \mathrm{DoD}^{\mathrm{bat}}_{k}) \leq E^{\mathrm{bat}}_{k}(t) \leq E^{\mathrm{bat}}_{\mathrm{opt,k}} \tag{2.17d}$$

Equations 2.17b and 2.17c are thus modified to:

$$\forall t : -E^{\mathrm{bat}}_{\mathrm{opt,k}}\alpha_{\mathrm{k}} \leq P^{\mathrm{bat}}_{in,k}(h, TD) \leq 0 \tag{2.18a}$$

$$\forall t : 0 \leq P^{\mathrm{bat}}_{out}(h, TD) \leq E^{\mathrm{bat}}_{\mathrm{opt,k}}\alpha_{\mathrm{out}} \tag{2.18b}$$

PtG limits makes a direct use of time-variable power:

$$P^{\mathrm{PtG}}_{\mathrm{inst,min}} \leq P^{\mathrm{PtG}}_{\mathrm{inst,opt}} \leq P^{\mathrm{PtG}}_{\mathrm{inst,max}} \tag{2.19a}$$

$$\forall t : -P^{\mathrm{PtG}}_{\mathrm{inst,opt}} \leq P^{PtG}(t) \leq 0 \tag{2.19b}$$

Equation 2.19b is thus modified to:

$$\forall t : -P^{\text{PtG}}_{\text{inst,opt}} \leq P^{PtG}(h, TD) \leq 0 \tag{2.20}$$

Please note that only the variable limits connected to the TD model were developed mathematically for more concision. An extensive explanation of these limits can be found in [34] section 1.4.3 .

2.3.4 k - medoids

The clustering method k - medoids has been explained in section 2.2 and this section will be discussing its implementation in our program.

Initialization Our program uses the k - medoid algorithm explained in section 2.2 to cluster multiple data sets. The input of this data is processed to include power consumption, wind velocity, solar irradiance and local hydraulic inflow. Each data distribution D is given a specific weight depending on the cell's topology/consumption profile and subsequently normalized. The distribution D to be clustered is defined as follows for every member of D, i in cell c:

$$\forall \text{ cells } c\text{: } D_i^{\text{cons}} = \omega_c^{cons} \times \frac{P_i^{\text{cons}}}{\sum_m P_m^{\text{cons}}} \tag{2.21a}$$

$$\forall \text{ cells } c\text{: } D_i^{\text{hydro}} = \omega_c^{hydro} \times \frac{P_i^{\text{hydro}}}{\sum_m P_m^{\text{hydro}}} \tag{2.21b}$$

$$\forall \text{ cells } c\text{, PV park } k\text{: } D_i^{\text{irr}} = \sum_k \omega_c^{irr} \times \frac{P_{i,k}^{\text{irr}}}{\sum_m P_{m,k}^{\text{irr}}} \tag{2.21c}$$

$$\forall \text{ cells } c\text{, WT park } k\text{: } D_i^{\text{wind}} = \sum_k \omega_c^{wind} \times \frac{P_{i,k}^{\text{wind}}}{\sum_m P_{m,k}^{\text{wind}}} \tag{2.21d}$$

Where parks represent the multiple PV, WT onshore and WT offshore parks available per cell.

Iteration Once this data distribution is composed, the program will run the clustering algorithm a fixed amount of times (given as input by the user) on this data set and will store the smallest error that every local optimum produced. This error is computed as the squared euclidean distance (equation 2.1) between the distribution point x and the medoid m divided by the number of cluster used:

$$\text{Error} = \sum_x \sum_m \frac{|x - m|^2}{NrTD} \tag{2.22}$$

Please note that the program has been adapted to support multi-threaded computations when choosing initial medoids thus increasing the speed of computation by a factor of two for a four-core processor.

This implementation results in a fixed number of TD's for the whole year, where every day possess it's associated TD for every cell in the system. This is illustrated in Figure 2.5 for a 12 TD system.

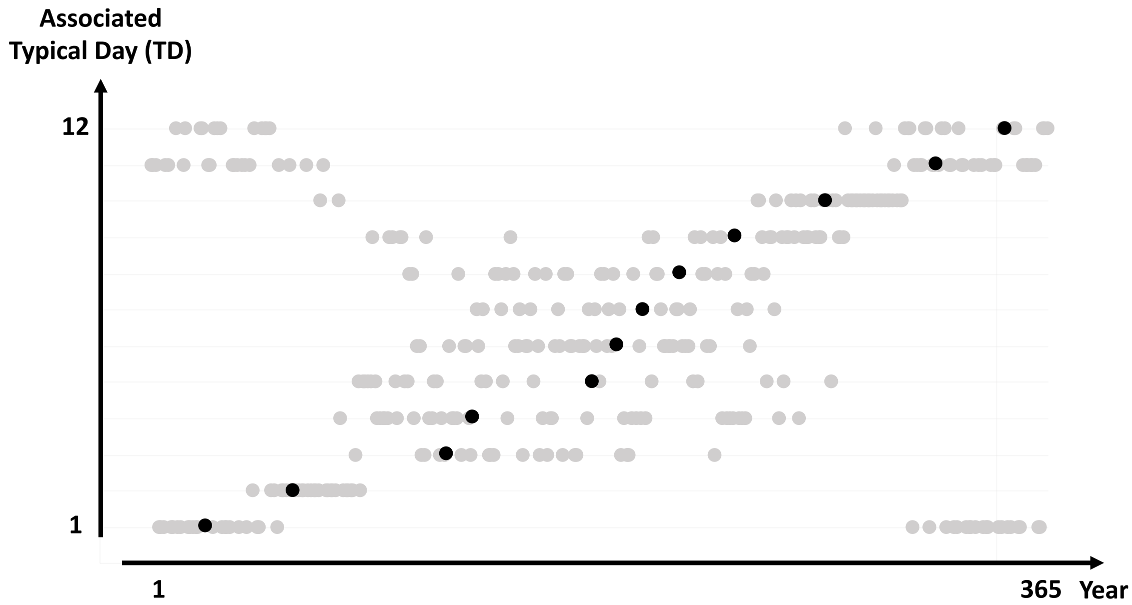

Figure 2.5: *Every day of the year (grey dots) associated to one TD (black medoids), adapted from [24]*

Systems implementation The implementation of this clustering on our different data sets can be performed through three methods that will articulate around the weight factor W.

The first method, gathers all the data under the same weight and performs a clustering on a uniform cloud of data sets. This method generates thus the weight factor of equation 2.21 as a unit vector. A first improvement can be easily achieved by considerably increasing the weight factor of the power consumption compared to the other meteorologic data sets. Indeed, power consumption is the only data set constraining every hour the power balance as described in equation 2.10. A factor of three is thus decided for the power consumption.

The following step that was undertaken was personalizing the weight factor per cell depending on their natural resources distribution. For example, Germany & Benelux will not take into account the hydraulic local inflow, whereas Scandinavia and Italy & Alpine States would have to take it into account given their high reliance on PHES, dams and runrivers. Whether the system is one cell, two cells or whole NWE, the distribution used is the same. The distribution per cell of the weight factor can be found in Table 2.1. Please note that the weight factor is normalized (since the sum of its elements does not add up to the same value for every cell) in order to avoid an artificial weight on the following cells: Scandinavia and Italy & Alpine States. These cells take hydraulic inflow into account.

Cells	Power	Irradiance	Wind	Hydro
Scandinavia	3	1	1	1
British Isles	3	1	1	0
Germany & Benelux	3	1	1	0
Italy & Alpine states	3	1	1	1
Iberian Peninsula	3	1	1	0
France	3	1	1	0

Table 2.1: *Weight factor ω for the different cells representing the data sets distribution for K - medoids*

2.3.5 Example: through a three TD week

In order to illustrate the concepts put forward in these sections, let's take an intuitive example with Figure 2.6. Assuming a regular week of two sunny days, three very cloudy days and two shady days, we will implement TD.

Instead of modelling those seven days independently, we will regroup these days by meteorologic profile and thus reduce the complexity. Those groups will be our TD. The model of this study is coupling the TD method of [30] and the energy constraints of [24] .

This figure highlights the difference between *power* and *energy* which is fundamental in the understanding of the TD model. As explained in the beginning of the section 2.3, the variation of energy (hence *power*) will be the same for every day associated to the same typical day (black line), but the *energy* (blue line) is different for every day of the week.

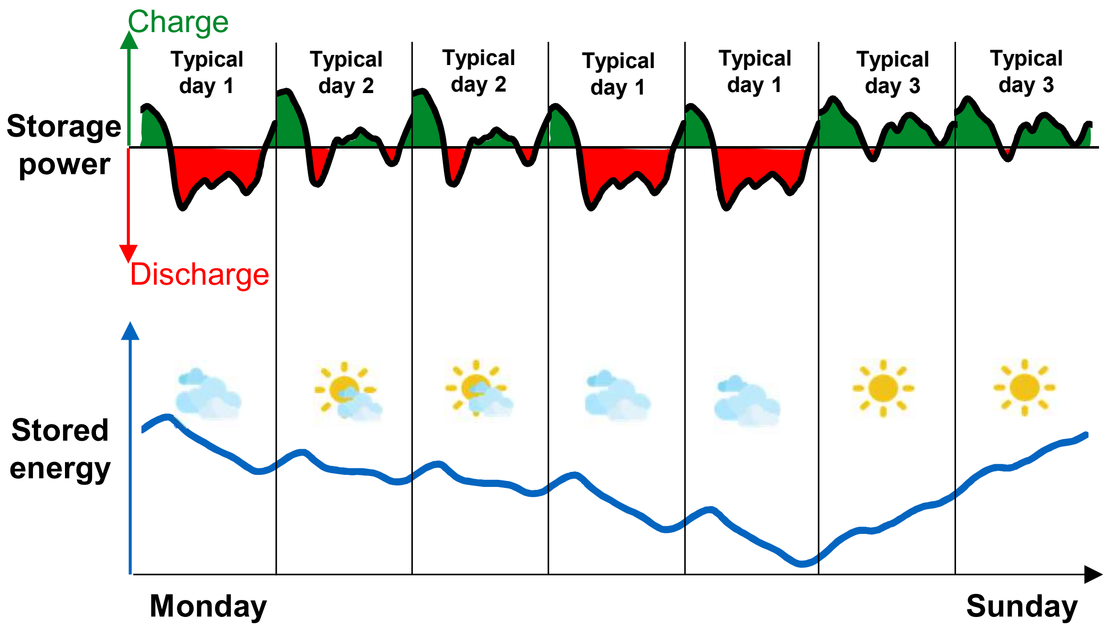

Figure 2.6: *One week of stored power and energy modelled by three typical days, from [24]*

Chapter 3

Validation

This chapter will validate the new program using the TD method compared to the previous work. Different parameters will vary and we will assess their impact on the simulations results. First of all, the number of clusters needed for the preliminary simulations will be tested and confirmed. Secondly, the clustering method will be validated within the parameters approximated: power consumption, irradiance, wind velocity and hydraulic inflow. Thirdly, the TD method will be cross-referenced with the reference case scenario in terms of the different production system and the objective function. This chapter's validation thus follows the reasoning of the program: one, compute the TD's and second, implement them into our LP.

3.1 Validation of k-medoids method in the EROI model

This section will assess the correctness of the implementation of the clustering program approximating the different parameters wanted and giving the TD as output. Please note that *clusters* will be used as a synonym for TD hereafter. The approximated inputs were decided with respect to the importance of their linked production systems (hence wind for WT for example). The approximated inputs are hereafter referred to as "time-series". This validation is operated on one cell and then two cells eventually to validate the clustering method for multiple cells.

To illustrate this evolution, please find in figure 3.1 the load duration curve of the cell British Isles for different numbers of TD. One can observe a convergence of precision with an increasing number of TD.

3.1.1 Time series validation

Power consumption The power consumption validation will be conducted under the form of a load duration curve (LDC). Indeed, comparing hour per hour the two consumption of our models would lack of clarity. The LDC illustrates instead the relationship between the generating capacity requirements and the capacity utilization, which should be very close for a similar consumption. It is regularly used for a clearer expression of the power consumption. This parameter has been found of paramount importance for the TD implementation [24]. The match between the TD model's consumption and the real British consumption is thus extremely important.

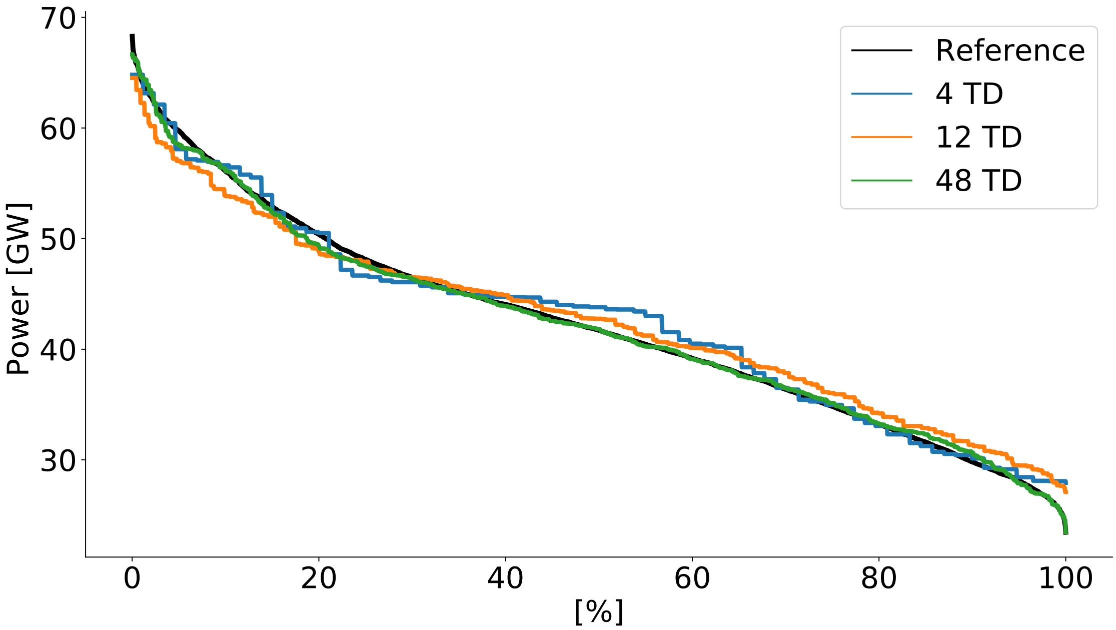

Figure 3.1: *Load duration curve approximation for different number of TD of the cell British Isles*

The load duration curve of a two cells system can be found in Figure 3.2. Please refer to Figure 2.2 for an example of cluster approximating it's corresponding power consumption in the British Isles. We can thus observe that our model approximates correctly, within an acceptable tolerance, the power consumption of our cell.

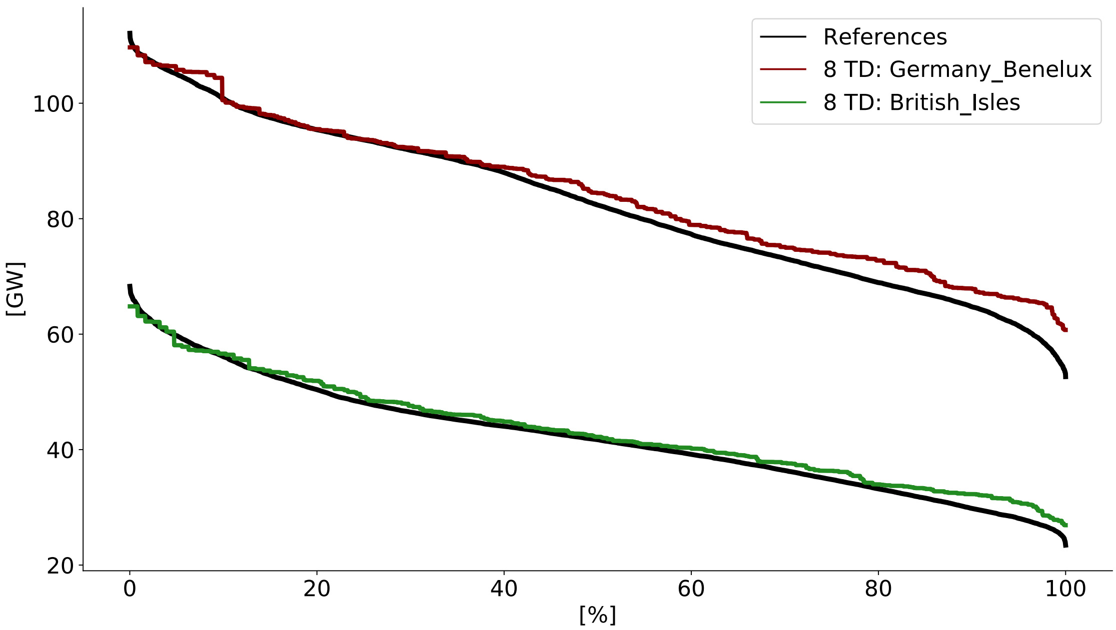

Figure 3.2: *Load duration curve expressing the percentage of use of the power generation capacity for two models: reference model [34] and TD model with 8 clusters*

Irradiance In the case of high RE scenarios, the approximation of sun irradiance is of prime importance. The clustering can be observed in Appendix B.3, where one of 5 TD is represented surrounded with the associated reference days (57 in this case). We can once more compare an irradiance duration curve in Figure 3.3 with a multiple number TD chosen. We can once again observe an accurate approximation of our model within the data to be represented as the number of clusters grow.

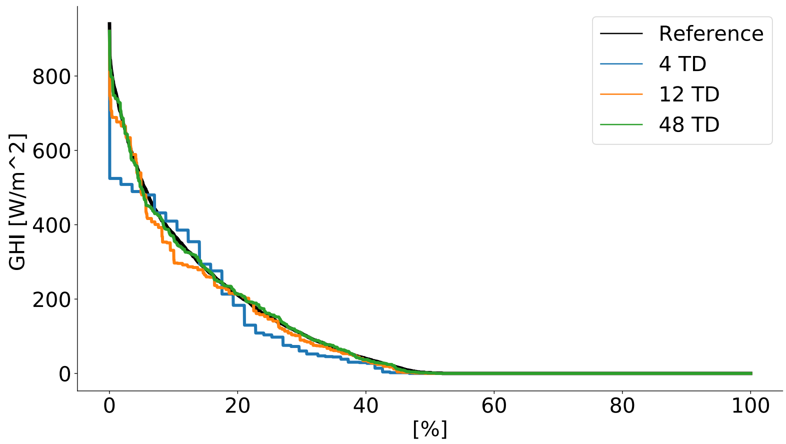

Figure 3.3: *Expressing the GHI (Global Horizontal Irradiance) data of reference and clustered in function of its occurrence*

Wind velocity In the case of high RE scenarios, the approximation of wind velocity is of prime importance. In order to validate this parameter, a wind velocity distribution was compared with the cluster's in Figure 3.4. Please note that the difference noted in the first percentage for 4 and 12 TD is indeed relatively high but, in terms of absolute precision, it represents a low error since these high winds occurs rarely. Furthermore, concerning WTs, these winds are already too high for the P_{nom}; it does not change their production. We can thus once again see a good approximation of of the system within the data to be represented.

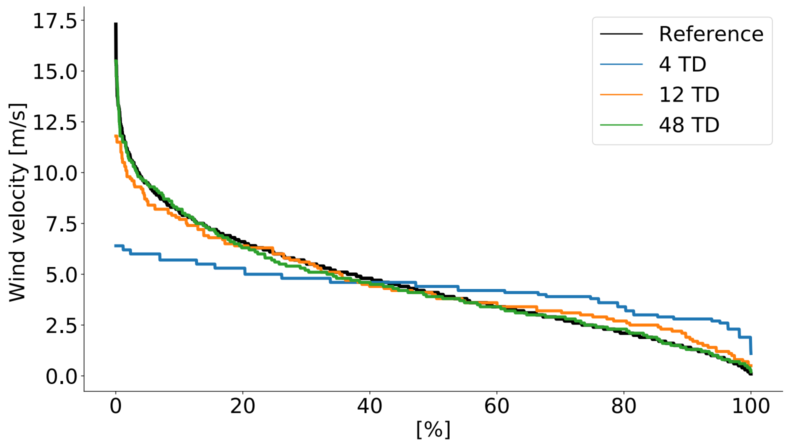

Figure 3.4: *Expressing the wind velocity data of reference and clustered in function of its occurrence*

3.2 Validation of the use of typical days in the EROI model

This section will compare exactly the solutions of our linear problem in the TD model and in the reference model through analyzing five distinct aspects: the objective function, the variables, the production systems, the energy flows and the computational time variances.

3.2.1 Objective function

A parameter has to be chosen to reflect the precision of the approximation. This parameter will be the objective function: the EROI. A fixed deviation of 5% from the reference case scenario is authorized on TD approximations. The comparison of different clusters in a system of two cells is shown in Table 3.1. Tables for the validation and the discussion of one cell can be found in Appendix B.1. As detailed in B.2, the clustering method of k-medoids seems to produce results with more deviation. This matter is further developed in the related Appendix. It is to be noted that 8 TD reflect a turning point in the two cells analysis of Table 3.1 where the number of clusters cannot reflect accurately the complexity of the problem.

One can observe the ***unusual*** values of the 48 TD's compared to the reference scenario. Surprisingly, they produce a very accurate objective function. This is further detailed in section 3.2.6.

Two cells	*Ref.*	*48 TD*	*24 TD*	*16 TD*	*12 TD*	*8 TD*	*Units*
Germany & Benelux							
PV	1,445	1,048	2,329	481	481	481	km^2
WT onshore	***11,085***	***31,271***	11,085	11,085	11,085	72,252	*WT's*
WT offshore	37,259	30,836	27,834	46,170	45,034	47,679	*WT's*
Batteries	***1,433***	***2,016***	731	1,033	295	1521	*GWh*
Power-to-Gas	160	244	138	228	177	428	*GW*
Gas storage	50	59	31	42	78	100	*TWh*
Curtailment	0	0	0	0	0	39	%
British Isles							
PV	127	127	127	127	127	127	km^2
WT onshore	48,839	45,702	47,413	45,422	51,114	40,932	*WT's*
WT offshore	1,277	1,277	1,277	1,277	1,277	1,277	*WT's*
Batteries	705	1,035	708	457	550	1,412	*GWh*
Power-to-Gas	198	187	200	192	197	172	*GWh*
Gas storage	41	59	33	24	38	100	*GWh*
Curtailment	0	0	0	0	0	1	%
E_{inv}	143.6	145	136.8	137.4	137.4	190.3	*TWh*
EROI	***7.6***	***7.68***	7.76	7.71	7.75	5.7	/

Table 3.1: *Results comparison of two cells (British Isles and Germany & Benelux) between the reference model and the TD model with a variable number of clusters*

Six cells As the six cells system shows a higher degree of complexity, attaining the 5% approximation is no easy task for a small amount of TD. The TD that have achieved this degree of precision are summarized in Table 3.2. More on the searching of TD for the six cells system can be found in Appendix B.3.

Six cells	Reference	46 TD	42 TD
E_{inv} $[TWh]$	349	349	363
EROI	8.5	8.6	8.2

Table 3.2: *Summary of the energy invested and the EROI for the reference scenario, 46 and 42 TD for the six cells system*

Unfeasible problems It is to be noted that as the number of TD decreases, so does the global precision of the approximation as stated in the analysis here above. Furthermore, decreasing the number of TD beyond this critical number of clusters generates unfeasible problems. Indeed, two clusters and four clusters generate a problem that is unsolvable for one cell and two cells respectively. This can be explained by the daily constraints on storage that may become impossible with too few different profiles (i.e. TD).

3.2.2 Variables

The core technique of the TD method to reduce computation time is to build a simpler problem for the solver. This is achieved by reducing the number of variables to be optimized by a factor proportional to the number of clusters chosen. The majority of optimized variables being a power metric, the TD method applies very well to this case. The only energy variables impossible to optimize are linked to day-to-day storage constraints. The decrease in variables is illustrated in Figure 3.5 and numerical values are for one cell with a time step of one and a number of TD of 12. Please note in these schematics that the differences between energy variables (whose boxes do not change in size) and the power variables decrease drastically. As a result we numerically observe a reduction from 131 thousand to 38 thousand variables, i.e. a reduction of 30%. Reducing further the number of variables would increase the gain in computation time but will not work with the inevitable energetic constraints for our storage.

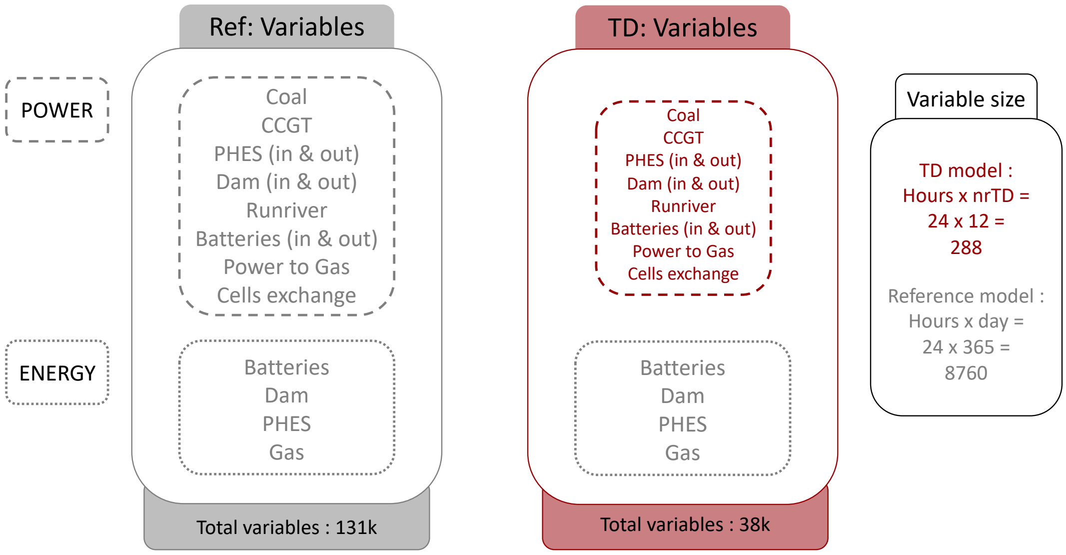

Figure 3.5: *The different number of variables of power and energy optimized in the LP seen through the reference model and the TD model. Illustrated for one cell, 12 TD and a time step of one.*

Systems The number of variables evolves with the number of cells. Hence the improvement of the TD method increases with complexity. Table 3.3 regroups the evolution of variables in function of the system and the number of clusters. One can easily observe the trade-off that has to be made between number of clusters (and thus increasing variables) and the complexity of the LP (and thus its precision). As a result we can see a sharp decline in numbers of variables in the TD model compared to the reference model hence validating the simplification of the LP. Please note a linear relationship between the number of variables and the number of TD, implying that an increase in the number of TD does not translate to a drastic increase in LP.

	Ref.	*48 TD*	*24 TD*	*12 TD*	*8 TD*	*4 TD*
One cell	158k	66k	59k	56k	55k	54k
Two cells	350k	138k	121k	113k	111k	108k
Six cells	1,472k	467k	391k	353k	341k	328k

Table 3.3: *Variation of variables in thousands of the LP in function of system and number of clusters (time step of 1).*

3.2.3 Production systems

In order to finalize this validation, some practical situations will be compared. The results of production matching consumption for one week with TD can be found in Figure 3.6. On this figure, one can notice a repetitive pattern for some days of the month. These patterns represent different days linked to the same day and thus using as approximation the same TD. Indeed, in this week, three days (first, second and last) possess exactly the same profile of production and consumption illustrating the TD model. Furthermore, this week illustrates very clearly the challenges of a 100% RE electricity grid; huge variations of power production from intermittent energy sources that have to be flattened throughout an expensive storage. Please note the high dependency on PtG for three days. While being at its earliest stages of development, when implemented in this type of LP, we can already observe a high reliance on long term storage such as PtG.

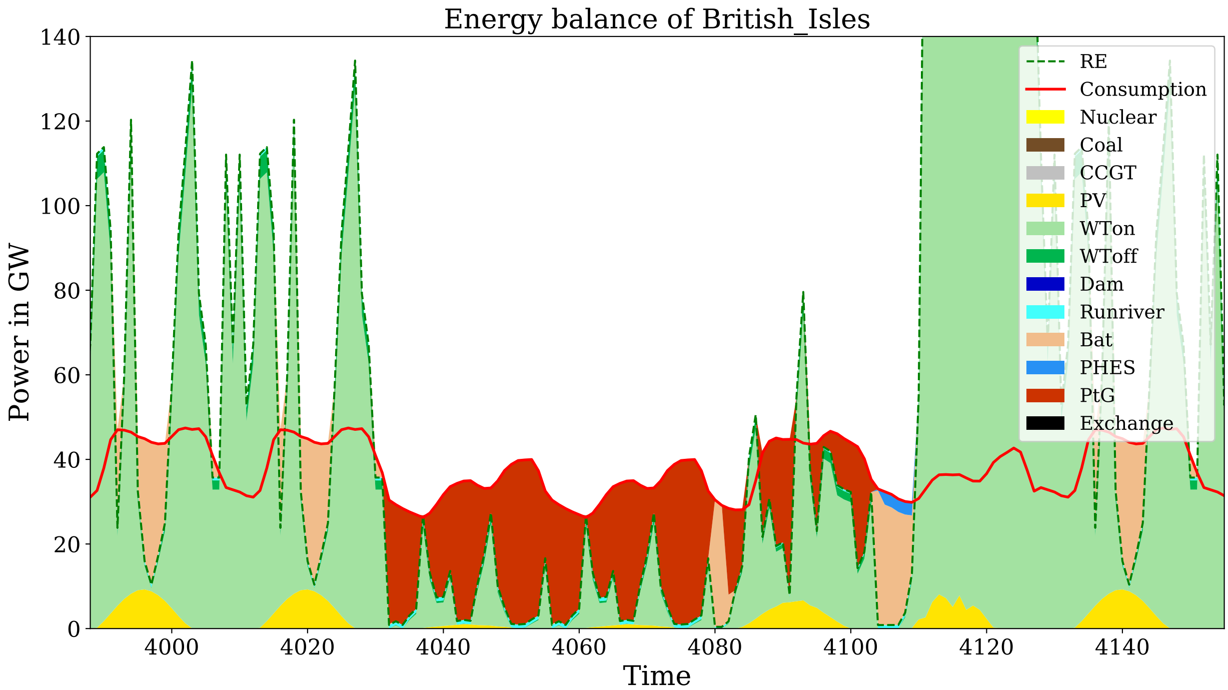

Figure 3.6: *Example of one week of power production in a 100% RE scenario with typical days with WT production peaks up to 300 GW*

3.2.4 Energy flows inside and outside the cells

Import and export Importing and exporting countries are compared in the two different methods. This is shown in table 3.4. Some small differences occur in the individual cells but global importing/exporting cells remain. Moreover, the total fluxes in the systems are very close. The reference case scenario has a total flux of 89.4 TWh while the TD method possess 86.9 TWh, a mere difference of 2.8 %.

Exporting cells [TWh]	Reference	12 TD	Reference share	12 TD share
France	56.9	50.4	9.5 %	7.7 %
Scandinavia	18.3	17.4	5.5 %	5.3 %
Italy & Alpine States	14.2	19.1	2.6 %	3.3 %
Importing cells [TWh]	Reference	12 TD	Reference share	12 TD share
Germany & Benelux	71.8	73	8.6 %	8.3 %
Iberian Peninsula	11.1	10	3.1 %	2.6 %
British Isles	6.5	3.9	1.2%	0.7 %
Total	**89.4**	**86.9**	/	/

Table 3.4: *Importing and exporting cells in the different models: reference and 12 TD in a 100% RE scenario*

Energy flows of one of the six cells The monthly energy flows of the cell Italy & Alpine States for the reference case and the TD method are illustrated in Figure 3.7. These were generated for a 100 % RE scenario in NWE with a time step of one. One can see that general trends are very similar: a seasonal PV production, relatively constant WT's production, seasonal dam production and a heavy reliance on the PtG storage technology.

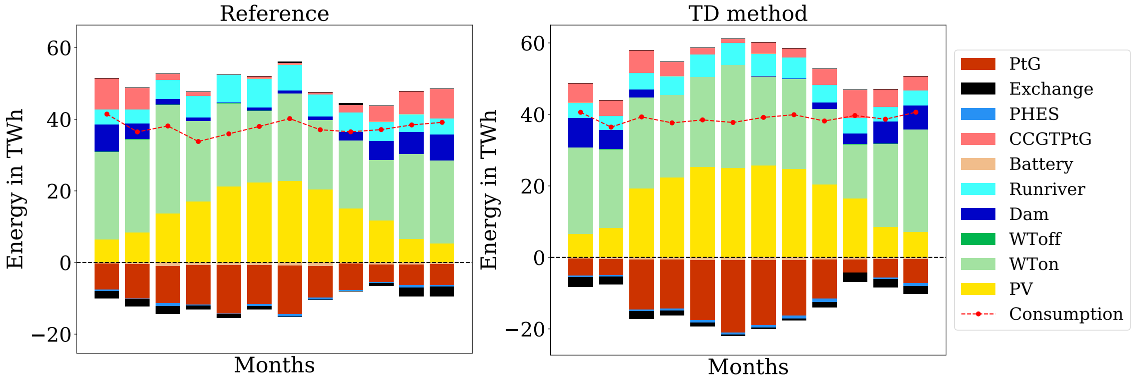

Figure 3.7: *Monthly energy flows of the cell Italy & Alpine States for the reference case scenario (1st graph) and the TD method (second graph) respectively*

3.2.5 Computational validation

The last part of this validation is conducted to validate the purpose of the TD method. Indeed, the first application of this method is the reduction in terms of variables of our LP. Since the number of variables is reduced (validated in table 3.3), so is the computation time. Time reduction will be compared for different systems, taking into account: the reference model, the fastest and the slowest clustering methods. A fixed tolerance of 5% of deviation from the objective has been set for clustering models before being accepted. Results are shown in Table 3.5.

One cell In the analysis of the British Isles cell, one can observe in Table 3.5 an increase in the solver's speed by a factor of 4. A higher order clustering leads to a slower computation speed. This system's simplicity (only one cell) allows for the use of a small amount of clusters staying within the fixed tolerance on the objective.

Two cells In the two cells scenario, 16 TD has been found as the fastest problem resolution with respect to the tolerance on the objective and the same proportion of means of production and storage as the reference case. We can thus see in Table 3.5 a reduction of 30% of computation time for the sixteen chosen clusters. Please note that choosing an unnecessarily high amount of clusters to solve this problem considerably slows the problem down. This can be observed here with forty eight clusters whereas sixteen clusters produce results inside our tolerance.

Number of TD As we can see, the fixed tolerance of 5 % of deviation from the objective of the TD' approximation puts a higher constraint than the "elbow" optimum described in section 3.1. More processing power than the optimum is thus needed to increase the precision of our TD model.

	Fastest TD	Ref share	Slowest TD	Ref share
One cell	4 TD	26 %	48 TD	44 %
Two cells	8 TD	30 %	48 TD	64 %
Six cells	24 TD	59 %	38 TD	130 %

Table 3.5: *Comparison of the share of time the TD method takes compare to the reference scenario for different systems*

3.2.6 Linear problem illustration

Some unexpected behaviours can be observed in certain TD results from tables 3.1. Indeed, taking as example the closest clustering resolution in terms of objective (EROI) in the two cells case (48 TD) we can see a huge difference in WT investments in the Germany & Benelux cell. This is linked to the construction of our problem as a linear problem which has a high sensitivity to slightly different inputs, please refer to [25] for more information on this topic. As an illustration to the odd behaviour of 48 TD, the boundaries of means of production have been set on our problem to match the reference's. More similar results in means of production were found with a slightly worse objective of our forced boundaries; a 1.3 % smaller EROI.

Chapter 4

Results: new scenarios

Since the newly elaborated TD method has been validated in terms of results and in terms of increased computation time in chapter 3, new results can be computed thanks to this new method and its new performances.

As the power system is highly influenced by political decisions [8], such as nuclear phase-out, taking into account these decisions into our model would be coherent. This would pave the way to questions such as: are the political decisions in phase with energetic optimization? Are national energetic objectives consistent with an optimized pan-European power system?

In order to generate realistic future scenarios, the energy policy of the studied countries has to be analyzed. All European Union (EU) members have a legal binding RE electricity target for 2020 in order to respect the 20-20-20 goals of the EU; 20% reduction in green house gas (GHG) emissions compared to 1990, saving of 20% of energy consumption and 20% share of RE in the European energy mix.

The EU has also set various energetic milestones to trigger a pan-European sustainable movement: a 40%, 60% and 80-95% reduction of GHG emissions, compared to 1990 levels, in respectively 2030, 2040 and 2050. [11, 12, 14, 15]

In order to analyze these future scenarios, several steps will be implemented. First, an exhaustive study of national commitments will be conducted (Section 4.1). Secondly an analysis of those commitments in a European plan will be studied (Section 4.2). Thirdly, the EROI model will be adapted to the commission's proposal and an analysis with results such as interconnection importance will be presented (Section 4.3). Finally a study will be conducted to analyze the evolution of the EROI with the share of renewables of the system (Section 4.4). This will be followed by a brief discussion concerning the approach to the new model and a conclusion (Section 4.5).

4.1 National goals

The vast majority of the mentioned countries have already drafted national 2030/2050 energy roadmaps but rarely mentioning their expected electricity generation per source. With the exceptions of Denmark and Germany, both setting ambitious targets, national governments have yet to propose precise electricity roadmaps.[3, 4, 22]

Fortunately, the European Commission drafted a 2016 update of the "EU Reference Scenario : Energy, Transport and GHG emissions Trends to 2050" simulating all the energetic aspects of every EU member every five years until 2050.[13] This

Cells [%]	2020	2025	2030	2035	2040	2045	2050
Scandinavia	/	/	82	/	/	/	/
British Isles	49	50	51	49	47	45	47
Germany and Benelux	36	38	42	43	45	51	54
France	28	32	35	36	42	46	56
Italy and Alpine states	46	51	54	57	60	66	71
Iberian Peninsula	44	50	61	64	73	80	87

Table 4.1: *Percentage of RE in the generation of electricity for every 5 years between 2020 and 2050*

reference scenario is not to be used as a precise forecast but is merely a trends projection given certain assumptions. These assume the achievement of 2020 targets (correct until now) and certain market conditions and policies adopted until 2014. This scenario has been modelled with the help of the member states and a European consortium. We can thus use this projection to decide the most relevant years for analysis.

These results, found in Table 4.1, may seem incoherent for 2050, where several cells operating on a 100% RE electric grid is to be expected. As an example, the British Isles suffer from a decreasing share of RE. This can be explained by an impressive 35% increase in consumption (between 2020 and 2050) that is met with a mix of gas and renewables. Indeed, gross renewable production increases slowly from 51 TWh to 55 TWh. It is then important to note several impressive countries regardless of their cells results. Denmark, Norway, Ireland, Austria, Spain and Portugal score an 80% share or higher. The only country who has a constant RE share in the electricity mix is Sweden from 2020 throughout 2050 due to their pledged electricity production through nuclear energy.

It is to be noted that Norway and Switzerland are included in this study but are not part of the EU. The Reference scenario therefore does not mention them, and a separate methodology has been used. In the case of Norway, a Norwegian study from the Institute for Energy Technology proposing three future scenarios has been adopted [21]. The scenarios predicted trends for Scandinavia in 2030, we thus took the scenario for Norway which was closer to the European Commissions trends for Sweden and Denmark. Concerning Switzerland, a detailed government 2050 roadmap for the electricity system and its nuclear phase-out has been used. [6]

4.2 Commission's proposal

By taking into account recent political and economical decisions, the European Commission has drafted a precise evolution of power production systems. A summary is presented in table 4.2. As precise boundaries to our problem have to be set in order to use our program, the following steps will be operated on the trends for 2030, year chosen for its numerous available data and its occurrence in a foreseeable future. This model will hereafter be named «*commission's proposal* ».

Whereas it is clear for every cell that the RE should grow, it is interesting to note in the commission's proposal the different approaches of the cells towards the evolution of non-RE. Indeed, two fundamentally different approaches were chosen by France on one side and Germany & Benelux with Italy & Alpine States on the other. France decides to almost exclusively produce its non-renewable electricity with nuclear PP's and leave the rest of the production to RE. Germany & Benelux and Italy & Alpine states on the other hand decides to produce the non-renewable electricity through gas and coal PP. As those two configurations fulfill their target, meeting consumption and demand, the constraints on storage facilities and power exchanges and thus their global efficiency may differ. These differences are analysed in Section 4.3.2. Complete data used for the commissions proposal can be found in Appendix C.1.

Cells [%]	Cons.	Nuclear	Fossil fuels	RE
Scandinavia	+23	12.7	4.3	83
British Isles	+12	24.9	28.2	46.9
Germany and Benelux	+0.3	0.5	57.4	42.1
France	+2	63.3	2	34.7
Italy and Alpine states	+2	1.8	43.7	52.5
Iberian Peninsula	+1	7.2	21.8	51

Table 4.2: *Increase in consumption of NWE in 2030 compared to 2020 and percentage of production systems in 2030 according to the EU Commission [13]*

As this scenario was implemented some assumptions were taken and the TD method was used in certain cases.

Assumptions As the program was developed, biomass was considered in the same production mix as CCGT PPs. This should not highly impact the results of these studies as they were still considered inside the gas imports through the CCGT PPs. Furthermore, one of the reasons the French cell was under a lot of pressure was due to the non-flexibility of the nuclear PPs. This is not entirely correct as the french nuclear PPs were specifically designed to allow for more flexibility than conventional plants. [10] The copper plate assumption in cells such as Germany & Benelux has to be taken care of in a more complex manner in the program. Indeed, while the nuclear phase-out allows for more flexible PPs, increasing renewables put the German electricity grid under high pressure, thus reducing its exporting capacity. [1]

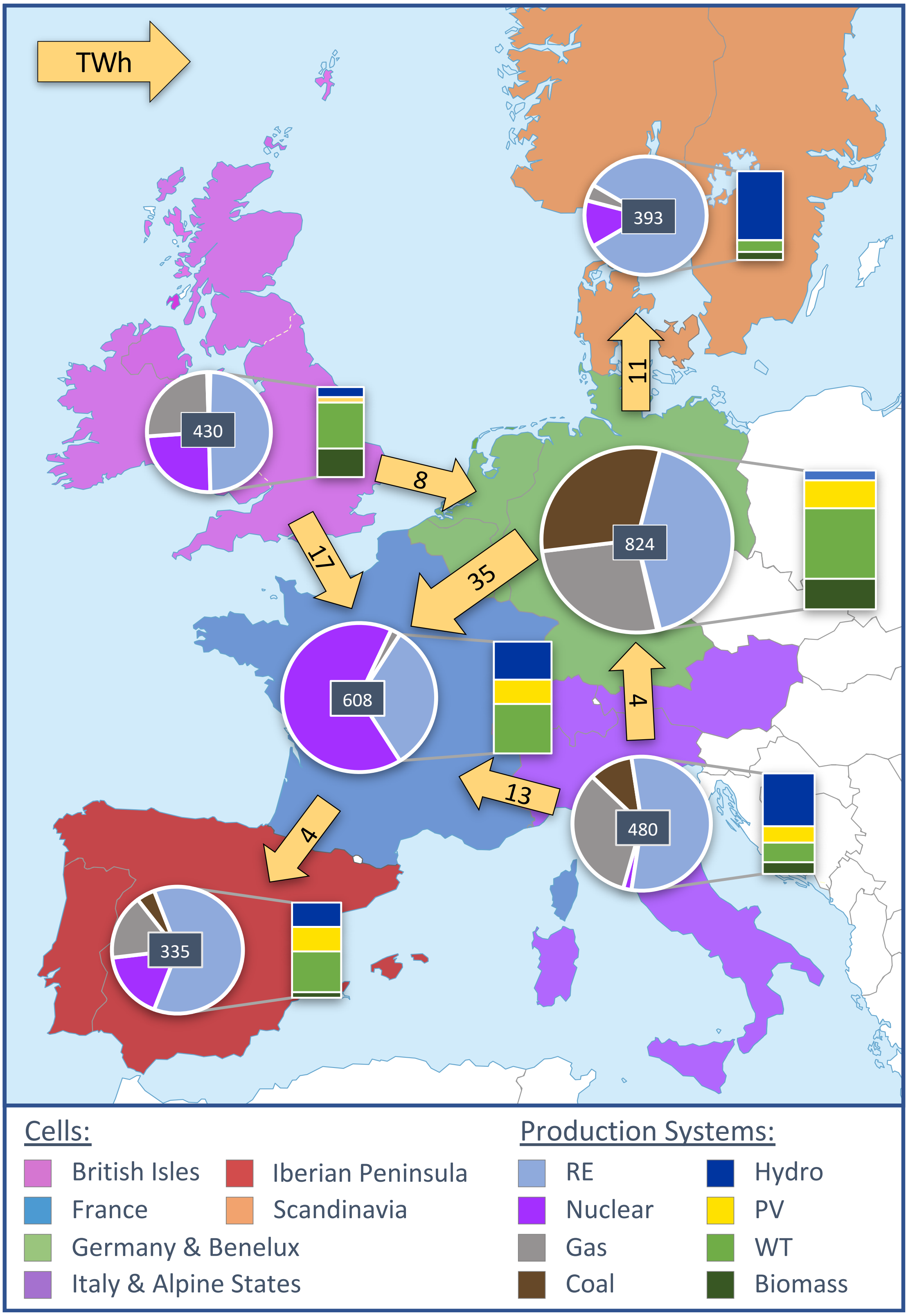

Figure 4.1: *NWE electricity generation system in 2030 with data of the commission proposal. Exchanges are expressed in the yellow arrows in TWh*

Typical day methodology The TD method has been used for rapid computation time for the constraints of non-renewable production systems on every individual cell. This significantly decreased the total computation time of the different simulations. However, once the systems complexity increases (such as six cells), a significant amount of computation time has to be poured into the research of TD for the system before beginning to solve the LP. This can be tedious for someone who doesn't have access to a high amount of processing power and thus this step has been overlooked for the EROI roadmap. The TD method is thus extremely efficient when working on a same system with the same input and changing problems which require a new resolution. The TD method then requires one long computation of TD and then allows for a high number of variances of the LP resolved in a simpler manner with fewer variables.

4.3 Scenario analysis

As comparison to the European commission's proposal, an altered version has been used with the EROI model, expressed hereafter as the "*EROI roadmap*". By fixing the non-RE production sources (nuclear, coal and gas) and taking the same installed assets, we can simulate the optimal RE's mix (with regard to EROI) to produce the rest of the electricity. The previous model has also been adapted to the estimated consumption of NWE in 2030 as shown in Figure 4.1. As the Commission's proposal does not mention any storage means nor power exchanges, they will be studied in the EROI roadmap in this section. Estimating their magnitude and constraints is of paramount importance to understand the NWE electric system of 2030. In order to verify orders of magnitude and as a first step, we will compare the two different systems constrained by the same non-renewable power production systems. Four analyses will consequently be conducted: the energy flows, the power exchanges in the system, the estimated emissions and an example illustrating the importance of interconnection.

4.3.1 Comparison between renewable production

By comparing the choices made on one side by the commission's proposal and on the other side by the EROI roadmap, we summarized the main differences in Table 4.3 .

Cells [%]	*WT*		*PV*		*Hydro*	
	EU	Adapted	EU	Adapted	EU	Adapted
Scandinavia	11	***19***	0	2	67	48
British Isles	25	19	3	2	6	3
Germany & Benelux	21	20	8	5	3	2
France	14	10	7	2	11	10
Italy & Alpine states	10	***20***	9	5	28	***18***
Iberian Peninsula	26	23	16	25	16	***6***

Table 4.3: *Comparison of the RE shares for the EU commission proposal (referred to as EU) and the EROI roadmap (referred to as adapted)*

As there are some differences (***highlighted*** in the table), the general trends remain very similar. We can thus make the assumption that the implementation of the EROI model with the Commission's constraints generates the correct trends. It is then correct to use this combined model in order to understand general trends such as imports/exports, storage and flexibility of the whole system.

4.3.2 Energy flows in EROI roadmap

Three different profiles in terms of energy flows have been deducted from the cells. The Iberian Peninsula, Germany & Benelux and France all had three different approaches to the electrical transition for 2030. These will be analyzed through this section. Please note in the upcoming energy flow diagrams that the difference between CCGT and CCGT-PtG. CCGT refers to imported gas which represents a conventional CCGT power plant and CCGT-PtG which refers to combustion in a conventional CCGT of gas generated by the PtG storage technology (and thus emissions free). The energy flows of the three remaining cells can be found in Appendix C.1 C.3 C.2.

Iberian Peninsula: The typical profile, found in Figure, 4.2 has a high RE share (more than half) coupled with a mix of conventional PPs. One can observe the high fluctuations of the conventional CCGT compensating for a very fluctuating seasonal PV production, thus highlighting the disadvantage of this technology. The Iberian Peninsula is also the only cell having implemented the PtG technology in order to ensure seasonal storage. Other cells also possess a high RE share (Scandinavia and Italy & Alpine States in Appendix C.2 and C.1), but do not require PtG because of their higher share of dams acting as seasonal storage. The exclusively onshore (no offshore) wind production of this cell may seem peculiar but can be understood by the means of two explanations. The first is that the inheritant characteristics of the problem are linear problem, as depicted in section 3.2.6. Secondly, the majority of the cell's coast is located in the Mediterranean, which has low wind speeds and its hydro-potential is low. This statement is justified in C.5. The cell's power sector is dominated by a large share of RE's that constrains the system as a net importer system with a large storage system.

Germany & Benelux: The profile depicted by the Germany & Benelux cell in Figure 4.3 represents a relatively low share of renewables with a particular electrical transition through the scenario studied. Indeed, Germany has decided to cut off its reliance on nuclear energy for a complete phase-out for 2030 of 141 TWh annual production (for 2010). As coal is a local natural resource of this cell, it is chosen as the alternative source of energy, thus explaining the fact that Germany possesses the highest share in NWE of coal PP [18]. Thus ,the power is based on conventional PP and the system does not require storage to support the integration of RE.

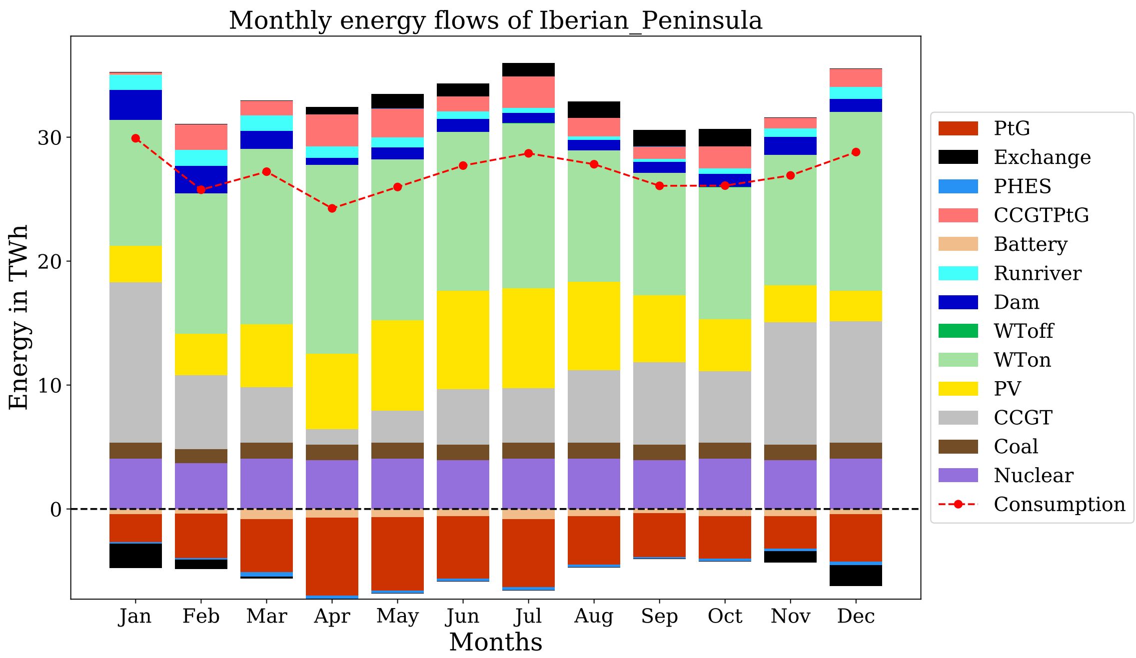

Figure 4.2: *Monthly energy flows of the cell Iberian Peninsula in the EROI roadmap*

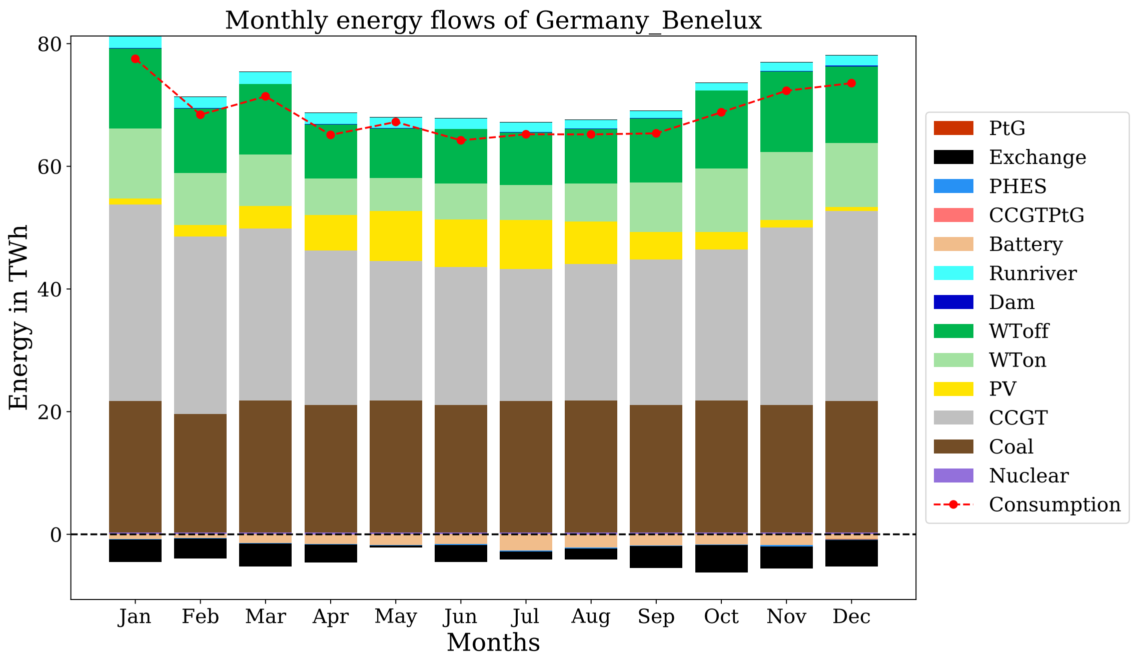

Figure 4.3: *Monthly energy flows of the cell Germany & Benelux in the EROI roadmap*

France : France's unique profile in NWE, illustrated in Figure4.4, presents a challenging national power sector for 2030. Indeed, a decreasing but still very high share of France's electricity is produced by nuclear energy inherently characterized by low flexibility. Coupling a very fluctuating yearly electricity demand with nuclear energy and a mix of renewables is very challenging for the system. Indeed, fluctuations are not being completely contained with the existing dams and batteries. These constraints force France to be the highest importer in the NWE system.

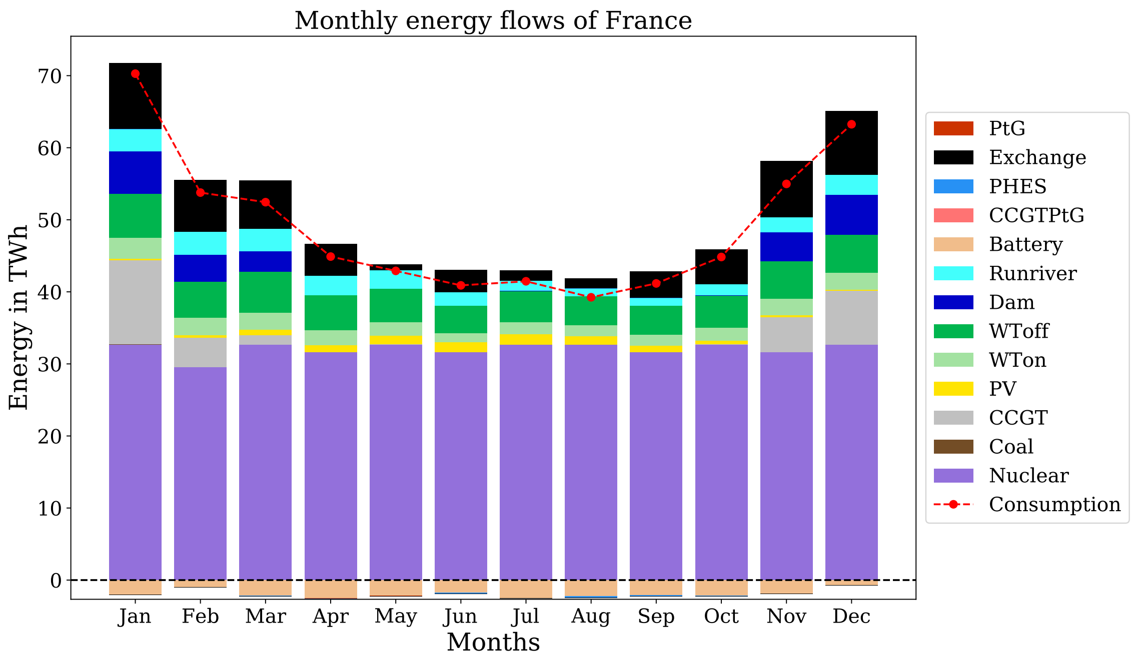

Figure 4.4: *Monthly energy flows of the cell France in the EROI roadmap*

4.3.3 Power exchanges

As the production mixes of the different cells differ greatly, an equilibrium of importing/exporting cells is defined. The exporting and importing cells with their share of coal and gas production can be found in 4.4.

Exporting cells	Net Export [TWh]	Export share	Gas and Coal share
Germany and Benelux	***35.5***	4.3 %	***56.9*** %
British Isles	24	5.3 %	26.3 %
Italy and Alpine States	12.8	2.6 %	42 %
Importing cells	Net Import [TWh]	Import share	Gas and Coal share
France	***59.1***	9.7 %	***3.3*** %
Scandinavia	10.7	2.7 %	5.4 %
Iberian Peninsula	2.4	0.7 %	21 %

Table 4.4: *Exporting and importing cells in the EROI roadmap with their export/import share. The correlation with their Gas and Coal share is highlighted*

For a six cell system, an equilibrium of three exporting and three importing cells has settled. Nevertheless, this equilibrium is highly unbalanced with 80% of the system's importations being France's cell. A strong correlation has been highlighted in 4.4 between the exchange and the gas and coal shares of the cell (as shown in **bold** in the table). By comparing this with the results of [34] for a 100% RE system, we observe that the trend is inverted as the Germany & Benelux cell was the largest importer in their model whereas in a mixed production system, it is the largest exporter. Indeed, cells tend to prioritize imported energy when issued from conventional PPs over investments in REs. This is highlighted in the case of the Scandinavian cell in the next paragraph. The energy fluxes through the largest importer and the largest exporter will also be studied. Indeed, France and Germany & Benelux interact with four other cells, being at the center of the system of NWE.

Scandinavian scenario: As illustrated in Appendix C.2 and in Table 4.4, Scandinavia seems to be a net importing cell every month. This can be surprising, knowing the high potential and already high pre-installed share of renewables. Indeed in the 100% RE scenario based on the same EROI model in [34], the Scandinavian cell is a net exporter with a very high EROI of 35. The energy flow diagram of the 100% RE scenario can be found in Appendix C.4. In the EROI roadmap, Scandinavia thus imports energetically cheap energy from Germany & Benelux instead of investing in their own renewables. This example illustrates the difficult challenge of cooperation between conventional, cheap power sources and to-be installed renewables.

France importer scenario: As we can see in Figure 4.5, France is every month a net importer but the absolute exchange varies greatly depending on the months. This behaviour mimics the fact that consumption is also highly season-dependant. Indeed, France's electricity system is highly sensible to variation in outdoor temperature[32]. The decrease in consumption during mild to high temperatures allows France to reduce the load of its importation. France exports during the months of spring and summer to the Iberian Peninsula whose consumption profile does not vary as much with the seasons. We can also see a constant unitary ratio of saturation on the connection between the British Isles and France. This can be explained by the attractive power of British Isles from an energetic point of view; a high share of non-RE pre-installed PPs with efficient RE production. The British RE production comes from onshore WTs with high wind potential (as seen previously in Appendix C.5) which is energetically interesting.

Germany & Benelux exporter scenario: Deeply linked to France with interconnections of a total 5.5 GW, Germany & Benelux's exports varies greatly with the seasonal demand of France, illustrated in Figure 4.6. Indeed, at the lowest point of France's demand, Germany & Benelux nearly achieves exchange equilibrium with only 0.3 TWh of exports in May. As in France, a constant unitary saturation ratio of the line between the cell and British Isles is also observed in import. This line possesses a capacity of 1 GW (named Nemo Link, discussed briefly in Section 4.3.5). A more variable export passes through the 2.15 GW connecting the cell and Scandinavia.

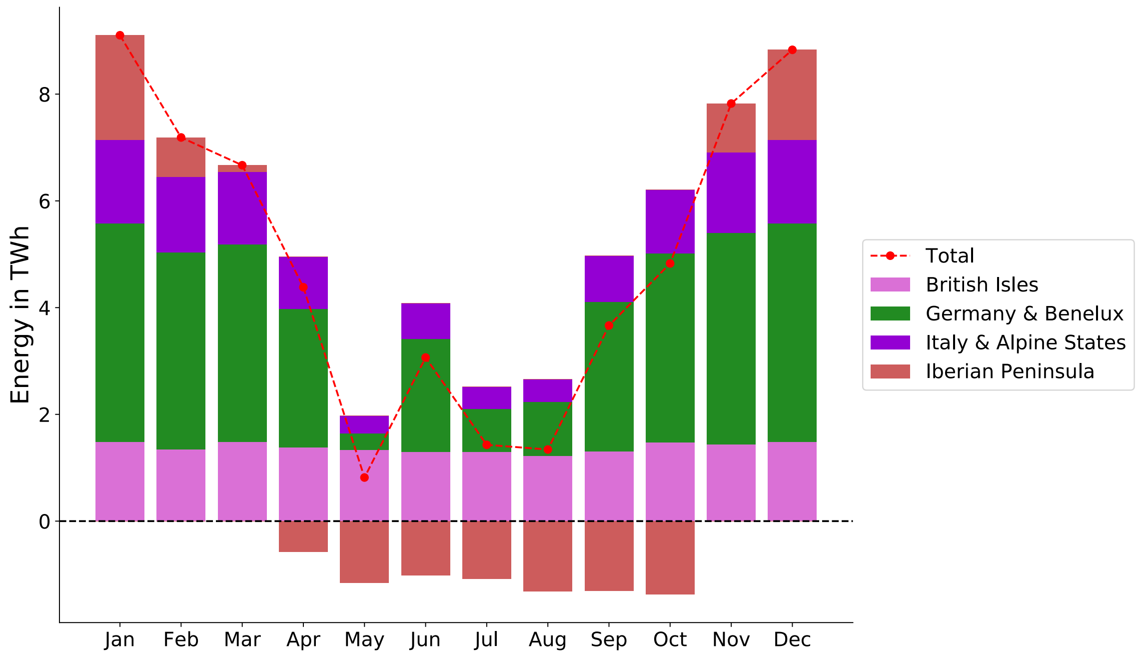

Figure 4.5: *Import/export balance of France with the other cells. Negative and positive values represent respectively export and import.*

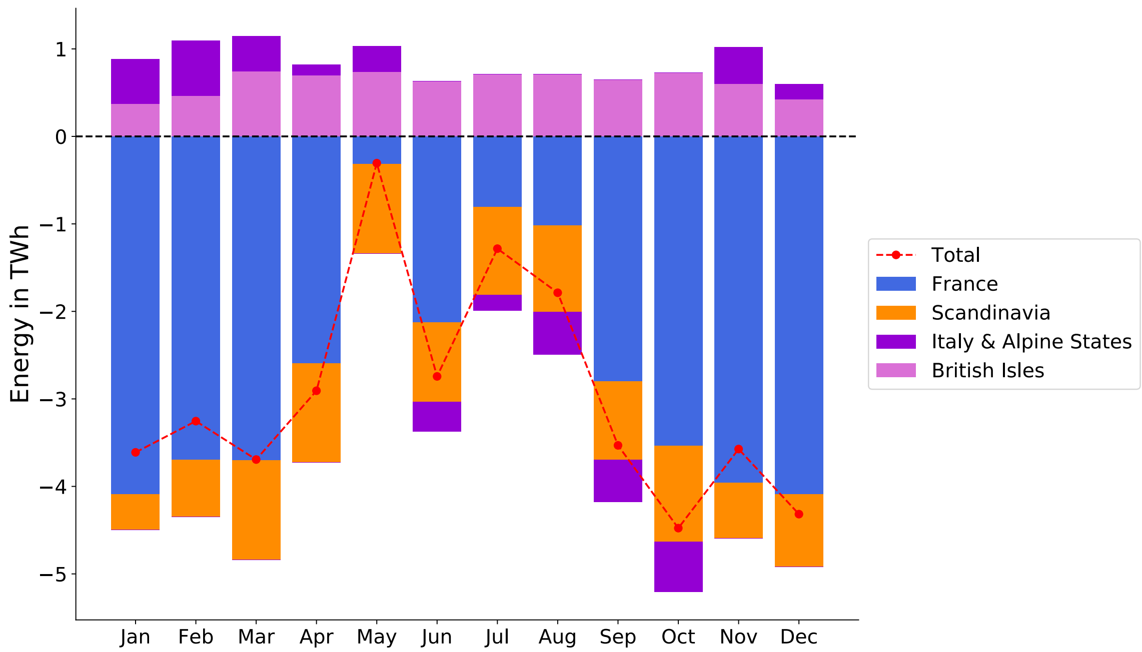

Figure 4.6: *Import/export balance of Germany & Benelux with the other cells. Negative and positive values represent respectively export and import.*

4.3.4 Emissions in EROI roadmap

Since the aim of study is to analyze a scenario in the context of the energetic transition, a brief emissions analysis is conducted in this section. Choosing a factor to represent the ecological impact of one's production system is no easy task. Because of its widespread use and its simplicity of implementation, CO_2eq. emissions will be used as metric to assess the ecological impact of this system. Please refer to extensive life cycle assesment (LCA)s on the ecological impact of the different types of PPs to have a complete understanding of the environmental impacts. The CO_2 emissions per production systems were found in the 2014 IPCC report [17] and are gathered in 4.5. More detailed emissions per production type can be found in Appendix C.2 .

gCO_2eq. / kWh	Coal	Gas	Nuclear	Biomass	WT	PV
Emissions	820	490	12	230	11	45

Table 4.5: *Emissions of the different production systems for electricity production. Issued from the 2014 IPCC report [17]*

As this data has been adapted to our case in Table 4.6, one can observe a decreasing global trend in line with the energetic transition but unfortunately lower than the 40% objective of the EU described in the introduction of this chapter. The impressive transition of British Isles is to be noted as the country completely backs out of coal-based energy production and focuses on electricity generation via nuclear, gas and WTs. The poor results of Germany & Benelux are also pointed out: a 54 % share of the total emissions of NWE for only 27 % of its consumption. However, phasing-out of nuclear energy without increasing its mean emissions still shows a high motivation to prioritize a de-carbonized electric system.

Cells	Emissions (MT)	Emissions share	Mean [g/kWh]	Actual [g/kWh]
Scandinavia	20	3 %	50	40
British Isles	78	12 %	***174***	***456***
Germany & Benelux	336	***54 %***	408	453
France	18	3 %	30	64
Italy & Alpine States	124	20 %	259	263
Iberian Peninsula	46	8 %	138	252
Total	622	100 %	***201***	***273***

Table 4.6: *Emissions in gCO_{2eq}/kWh of the different cells in: gross, share of total system, mean production and the actual production of 2019 (OECD data)*

4.3.5 Analysis of the cost-efficiency of an additional interconnection: Nemo link

The Nemo link is a recently installed connection between Belgium and England. It has a capacity of 1 GW and has been implemented in the previous computations in the EROI roadmap. Is this connection worth the cost ?

The EROI roadmap has been ran with and without this connection to assess its impact and importance. As shown in Table 4.7, one can observe the high impact on the system as the connection begins a process to even the exchange balance of Germany & Benelux and is constantly used at near unitary saturation rate. As the whole network is interconnected and every cell is impacted, this small connection disturbs up to the Iberian Peninsula who exports 200 GWh more than where there is no direct link. This highlights the increasing importance of the interconnection of NWE and proves the high cost-efficiency of this new line.

Exporting cells	Export without Nemo [TWh]	Export with Nemo [TWh]
Germany and Benelux	***43.1***	***35.5***
British Isles	16.5	24
Italy and Alpine States	12.7	12.8
Importing cells	Import without Nemo [TWh]	Import with Nemo [TWh]
France	59.5	59.1
Scandinavia	10.5	10.7
Iberian Peninsula	2.2	2.4

Table 4.7: *Exporting and importing cells in the EROI roadmap with their export/import share with and without Nemo link (1 GW line between UK and Belgium)*

4.4 Transition to a 100 % RE North West Europe

This section will study the evolution of the NWE system from the Commission's proposal to a 100 % RE system. While the the study in Section 4.3 thoroughly went over the response of our system, in this part we will look at a more macroscopic view. The evolution of the system will be studied at some important mile-stones: 45% (nearly the share of the EROI roadmap which is at 43.8 %) , 50 %, 60 %, 70 %, 80 %, 90 % and 100 % of renewable energy in the power system of NWE. These constraints were imposed on NWE as a global system and not on each individual cell. For example, imposing a RE share of 80 % on the system could produce a 60 % RE share in France and a 100 % share in Scandinavia. The rest of the system is un-constrained and the program optimizes the global EROI of NWE with the fixed RE share. The first part of this section will directly compare the EROI with the system's share of renewables, secondly we will analyze the roles of the different cells in attaining the desired global share and finally we will analyze more precisely certain interesting specific cases.

4.4.1 EROI variation to a 100 % RE system

As the RE share varies in the system, so does the global EROI. We will use the EROI parameter as metric of the difficulty for one's cell or system to implement the desired share of renewables. Hence, the more a cell or system has to invest for every unit of energy produced the more it will be reluctant to implement this solution. Please find the results of this study in Figure 4.7.

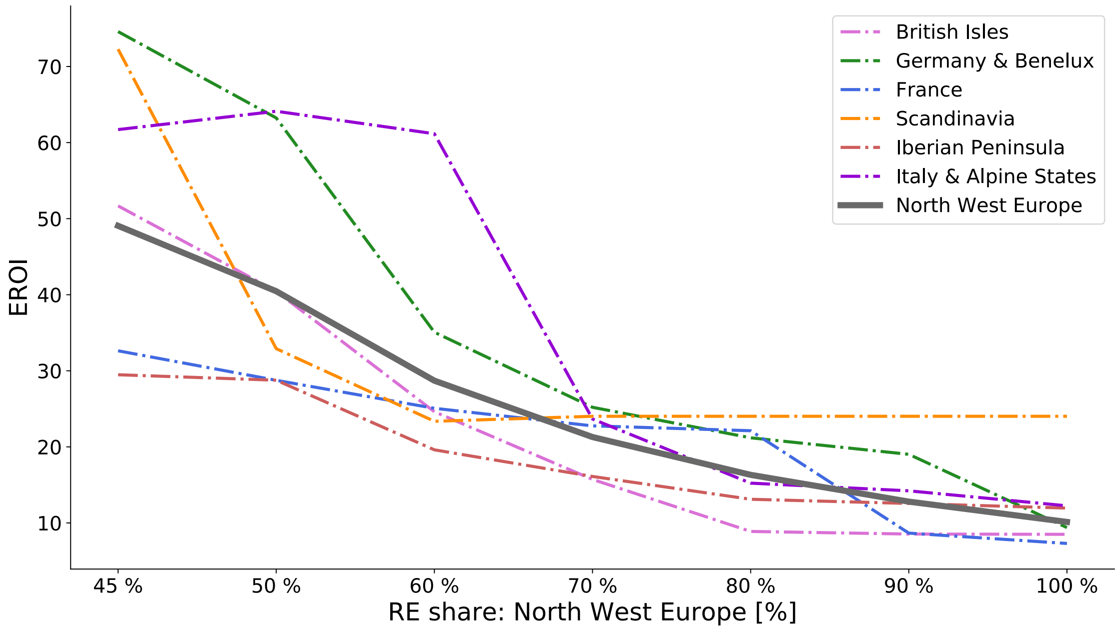

Figure 4.7: *Evolution of the EROI of the cells and the system in function of the percentage of renewable in the Norht West Europe system*

As a decreasing global trend can be observed from an EROI of 49 to 10 through the whole study scope, one can observe that the cells do not react homogeneously. Two types of slopes can be depicted on this graph: one steep decrease between 45 % and 70 % and a constant decrease between 70 % and 100 %. Each of the three intervals of the first slope are characterized by a sudden decrease of EROI in one of the cells: Scandinavia, Germany & Benelux and Italy & Alpine States respectively. The second type of slope of the system's EROI is characterized by more constant decreases of every cell. The specific cases of Germany & Benelux, Iberian Peninsula and Italy and Alpine Sates.

4.4.2 Macroscopic evolution of the different cells

As the constraints on the different scenarios of renewables share become higher, the different cells react differently to fulfill the system's constraint. Please find in Figure 4.8 the RE share of each cell in the system for the different scenarios. Some obvious patterns can be recognized. The smallest RE constraints are driven by Scandinavia and the Iberian Peninsula, that possess early on a high share of renewables. Those two cells are joined at 80% of the system's RE share by the British Isles and Italy & the Alpine States. In the last RE increases of the system, France and Germany & Benelux clearly fall behind with big increases in their RE capacity only at the

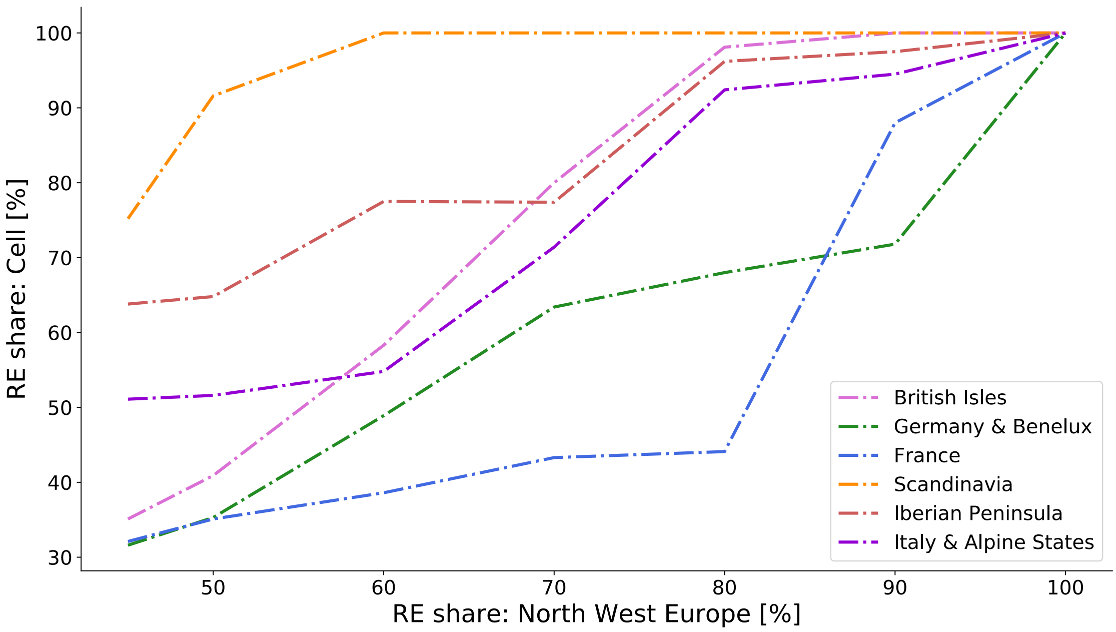

Figure 4.8: *Evolution of the RE share of each cell with the global RE increase of North West Europe*

very end of the study. Two types of slopes can also be depicted in this figure: France and Italy & Alpine States increase at once whereas cells such as the Iberian Peninsula and Germany & Benelux increase in two times. It is also important to note the general reluctance of the different cells to reach 100 % of renewables as they mainly stagnate around 95% before being forced to 100%. This shows once more the difficulty to "reach the last mile" as the energetic costs are high in these scenarios.

For more a more global view of each cell in the total system, please refer to Appendix C.6, illustrating the *relative* RE share of each cell in the system.

4.4.3 The energy transition in the different cells

The Figures 4.7 and 4.8 show some important variations in EROI and RE respectively between different scenarios for multiple cells. As these high variations seem impressive, it is important to keep in mind that the non-conventional PP are supposed pre-installed and possess thus no investment costs, explaining the high EROI in the early stages. It has been chosen to analyze more precisely four variations. A further analysis has thus been conducted on Germany & Benelux between 90% and 100%, the Iberian Peninsula between 50% and 60%, Italy & Alpine States between 60% and 70% and on France between 80 % and 90 %. As those intervals show great EROI and RE variations, understanding the correlation between these two metrics is of paramount importance. Indeed, as the EROI is defined as the total energy consumed on the total energy invested, a high variation of this parameter is translated as high/low investments as the energy consumed is constant. This is shown as a change in RE share and thus in the energetic mix of the cell.

Germany & Benelux As we can observe in Figure 4.9, the energetic behaviour of the cell changes drastically between a system scenario of 90 % and 100 % of renewables. Indeed, the cell has massive investments to make in both PV and WT offshore in order to compensate for the loss of its flexible CCGT and coal PPs. As these renewables lack of flexibility, the cell has to invest in a large PtG facility. As those investments are high for Germany & Benelux, the system of NWE avoids them for all the scenarios until it has no other choice in the 100 % renewables scenario. One can note that for high RE scenarios as studied here, Germany & Benelux has a net importer profile opposed to the biggest exporting cell of the system in the EROI roadmap.

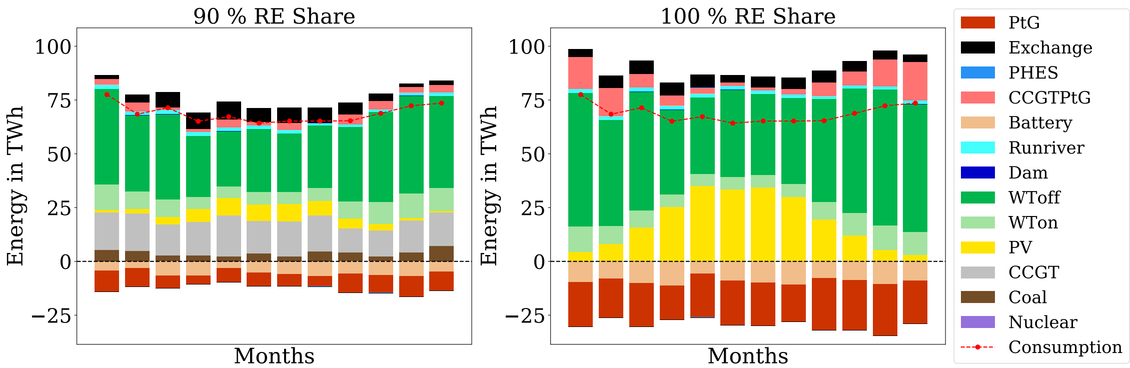

Figure 4.9: *Energy flows of Germany & Benelux for a 90% (1st graph) and 100% (second graph) RE scenario respectively. The cell's RE share is respectively 72% and 100%.*

Iberian Peninsula As one can see in Figure 4.7, the Iberian Peninsula undergoes high investments between the scenario of 50 % and 60 % of renewables (translated from a high variation of EROI). By analyzing in depth the monthly flow of the cell between the both scenarios in Figure 4.10, one can see the phase-out of nuclear. Indeed, for a higher RE share, the first conventional PP to be discarded is nuclear because of its lack of flexibility. This choice thus demands for high investments as the new onshore WT has to be backed-up with an increased facility of PtG.

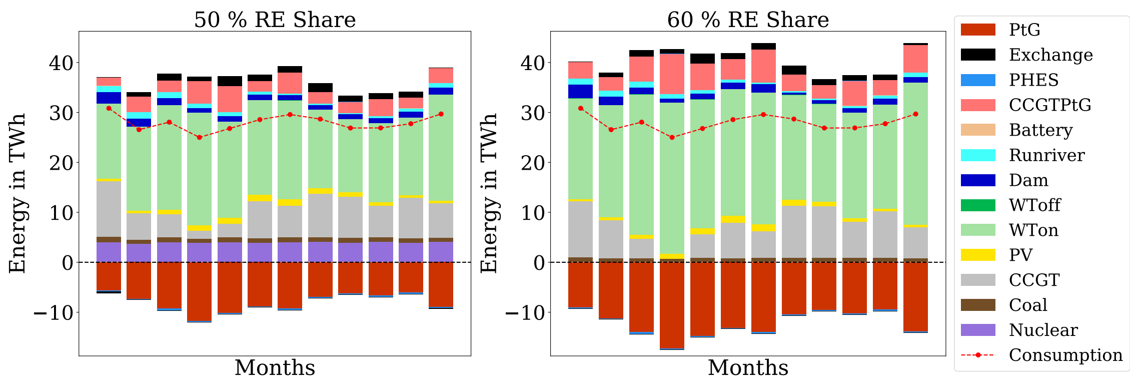

Figure 4.10: *Energy flows of Iberian Peninsula for a 50% (1st graph) and 60% (second graph) RE scenario respectively. The cell's RE share is respectively 65% and 78%.*

Italy and Alpine States As the system passes from 50% to 60 % of renewables in Figure 4.11, the cell Italy & Alpine States is unable to increase its share of renewables by keeping the same means of storage (dams). The variation of EROI in the Figure 4.7 was thus due to a high investment to install PtG facilities. As the new onshore WT are installed, the total production per month increases drastically compared to the previous scenario. This can be explained by the intermittent production of renewables.

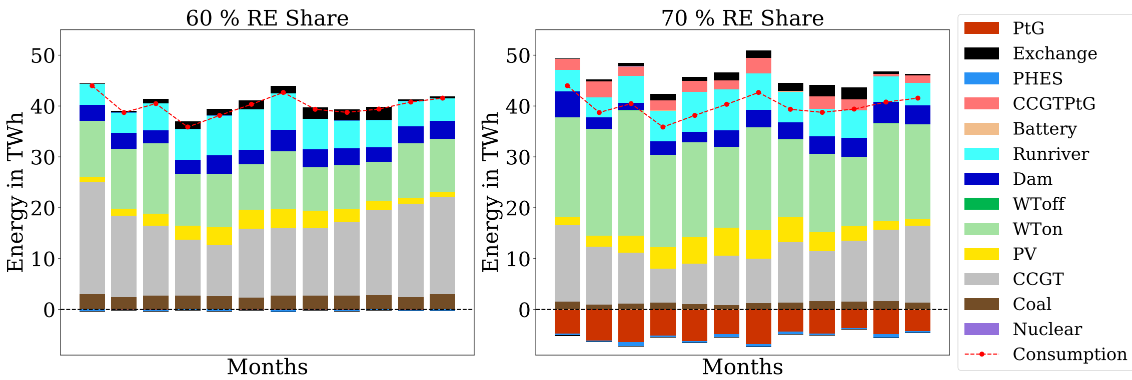

Figure 4.11: *Energy flows of Italy & Alpine States for a 60% (1st graph) and 70% (second graph) RE scenario respectively. The cell's RE share is respectively 55% and 71%.*

France As France doubles its RE share between two scenarios (from 44% to 88%), the energetic mix of the cell changes drastically. As we can observe in Figure 4.12, nuclear energy has shrunk from a 50% share to a mere 10%. As this production is replaced with a tripled PV capacity and a doubled number of offshore WT, the toll on the energy investments is high. Indeed, these renewables are coupled with an impressive battery park and an increased PtG facility.

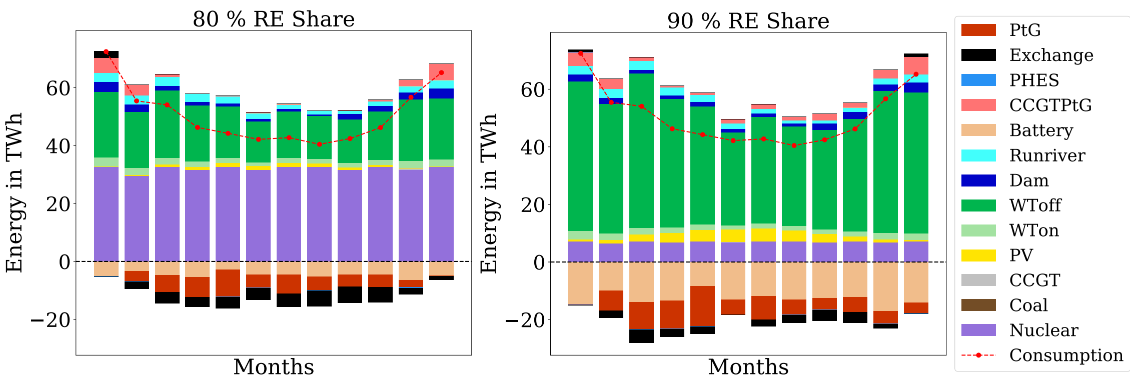

Figure 4.12: *Energy flows France for a 80% (1st graph) and 90% (second graph) RE scenario respectively. The cell's RE share is respectively 44% and 88%.*

4.5 Discussion and conclusion

Several important conclusions can be highlighted through the different studies conducted concerning the NWE system in this chapter. As it is clear that multiple energetic objectives have been set independently by multiple countries in NWE, a coherent approach was difficult to find. Fortunately, the European commission is willing to closely follow the consistent approach in order to find its optimum configuration. It has thus drafted a reference scenario for electricity trends up to 2050 every five years, taking into account recent energetic, political and economic decisions. This reference scenario has been adapted into our EROI model in order to conduct in-depth studies.

By fixing the non-RE production sources provided by the commission's proposal, the EROI model simulates the rest of the interactions and constraints in order to optimize the EROI of the system. Some differences were spotted for Italy & Alpine States and the Iberian Peninsula in the two models' share of the remaining non-constrained renewables, but the general trends settled.

Some observations are made from the energy flows of the three studied cells. With more than half of its electrical production produced by RE, the energetic mix of the Iberian Peninsula is highly diversified. Indeed, it is the only cell combining gas, coal, nuclear and renewables with PtG storage. As Germany & Benelux have decided through political decisions to produce a large quantity of its electricity with coal and gas PP, it has the possibility to export up to 35.5 TWh, 4.3% of it's production. On the other hand, France's high share of non-flexible nuclear production and intermittent RE cannot fulfill the demand on its own. This situation leads to a monthly net importer profile with a total import of 59.1 TWh, 9.7 % of its production. These import/export balances led to the correlation between the import/export share and the gas and coal share of a cell, highlighted in Table 4.4. Indeed, the more a cell imports, the lower their gas and coal share and the more a cell exports, the higher their gas and coal share.

The emissions analysis show a decreasing trend for the NWE system. The most impressive emissions decrease per kWh is the British Isles; from 456g to 174. This is contrasted by Germany & Benelux who accounts for 54 % of the emissions whereas they represent 27 % of the consumption.

The analysis of the new interconnection, Nemo link, highlights once more the energetic cost-efficiency of an interconnected NWE system.

Finally, the system with the installed non-conventional PP of the European Commission has been analyzed with a variable RE share on the system. A global decreasing trend of EROI is observed with an increasing share of renewables, highlighting once more the challenge of the electrical transition. Different electrical transition approaches were observed: an abrupt transition to 100% RE such as Scandinavia and France or the two stage transition of Germany & Benelux and the Iberian Peninsula. Four electrical transitions were compared: the full RE cell of Germany & Benelux, the nuclear phase-out of the Iberian Peninsula, the introduction of the PtG storage technology in Italy & Alpine States and the doubling of France's RE share.

Conclusion

As the need for efficient MES models grows with the energetic transition in Europe, two objectives were set. The two objectives to be fulfilled by this master thesis were 1) implementing and verifying the consistency of the new model resorting to TD and 2) analyze the energy transition of NWE.

In order to achieve the first objective, this study started on the EROI model developed by [34] (presented in Chapter 1) and proposed the implementation of the TD method to enhance the model (discussed in Chapter 2). The consistency of the implemented method (detailed in Chapter 3) was proven by comparing macroscopic systems metrics such as EROI and energy invested. During this validation, decreasing computation times were confirmed for the TD method compared to the reference model proposed by the initial study.

By applying the new method on the EROI model, the second objective could be fulfilled. Indeed, the energy transition of NWE was studied by starting from the European Commission's scenario for Europe (in Chapter 4). By applying the data of this scenario in the new model, consistency was verified with a known case. Subsequently, the study analyzed the energy transition of NWE. Three important aspects are highlighted: the strong correlation between the share of conventional PP and the export balance, the huge importance of additional interconnections and the correlation between the decreasing EROI with increasing renewables.

While this study was conducted, some limitations were encountered. The k-medoids method produced limited results in terms of error of the typical days for large systems. A more efficient clustering method could be implemented since the model must not be adapted for a change in the clustering method. This would allow for more complex simulations, taking into account more realistic parameters such as: an increased number of cells, the inclusion of the heat system or a better modelization of nuclear, coal or RE assets (such as biomass).

As much as the enhancement of this model would certainly be of great interest, the results of this master thesis already bring forward some alarming questions. Indeed, as the correlation between exchange capacities and the non-RE share has become clear and the causality between exports and GDP per capita has been proven, one can question the real implementation of RE in the current liberal power systems [26]. This concern is reinforced by the decreasing trend of the EROI with the increasing share of renewables. Will there be a common political front for the implementation of RE in NWE with discouraging energetic prospects (considering the EROI) and economical prospects (considering the import/export balance) ?

Appendix

Appendix A

Methodology appendix

A.1 Changes and validation of the EROI model

A.1.1 Changes

The EROI model used in this study is very similar to the one used in [34] and their program is available here: `https://github.com/sramelot/memoire2018` (new program is forked in Github). Two errors have been spotted and three precisions have been added for more realistic approximations.

Errors The two errors concerned local inflow and the run-of-the-river energy production. The first was omitting a max limit on the run-of-the-river variable producing unrealistic results in some simulations. This correction is in the initialization in the document "*lp_problem*" (line 93). The second error was the initialization of the local inflow before normalizing it to the annual production. This can be found in the class "*producers*" (line 188-189 and 214-215).

Precisions While the power curve of the wind turbines in the previous program was computed as a sum of an exponential between the cut-in and cut-out wind speed, the new method suggests an approximation with cubic splines. This has been modified in the class "*Producers*" (line 96 - 120). A comparative illustration can be found in Figure A.1. The cut-in, rated and cut-out speed have been respectively set at 4.5, 14 and 25 m/s. One can observe the smoother transition between the increasing curve and the rated speed for the cubic splines approximation. The compared WT is the Enercon E82/2300 whos power curbe is illustrated in Figure A.2. This change affects the system in the power generation for WT's but does not change fundamentally the different global trends.

Two other precisions were the irradiance and wind velocity variance in function of the load factor of the respective power system. The previous method used an iterative method with a fixed tolerance of 1e-3 whereas the new method computes those variables as the solution of a system resolved with the build-in function *fsolve*. These precision have been modified in the class "*Producers*" (line 96 - 120 and 42 -58).

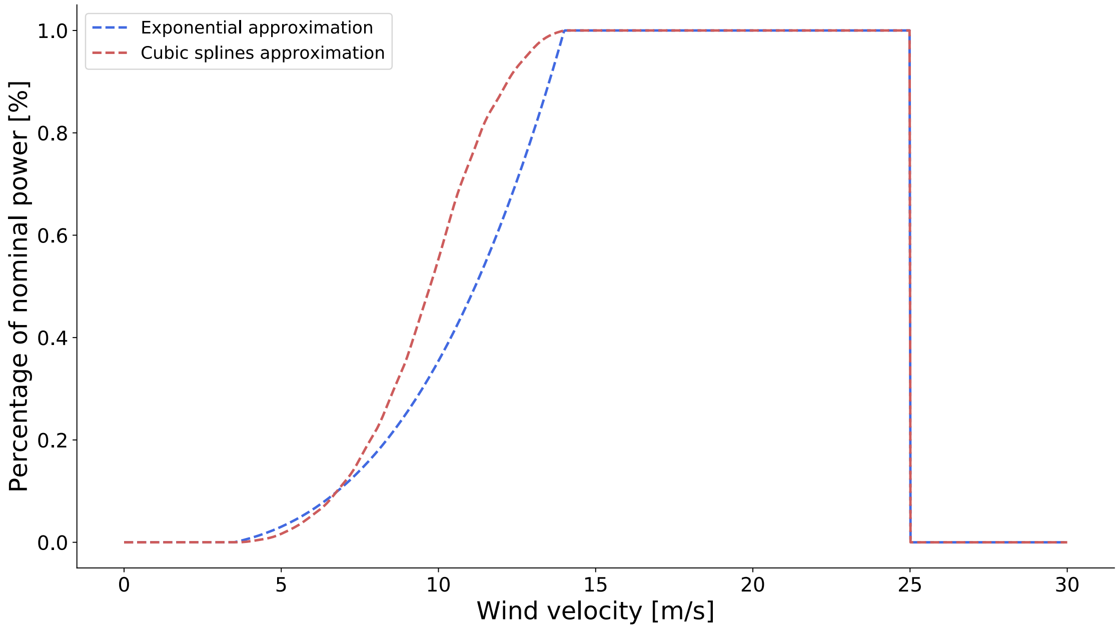

Figure A.1: *Power curves of the two different approximations*

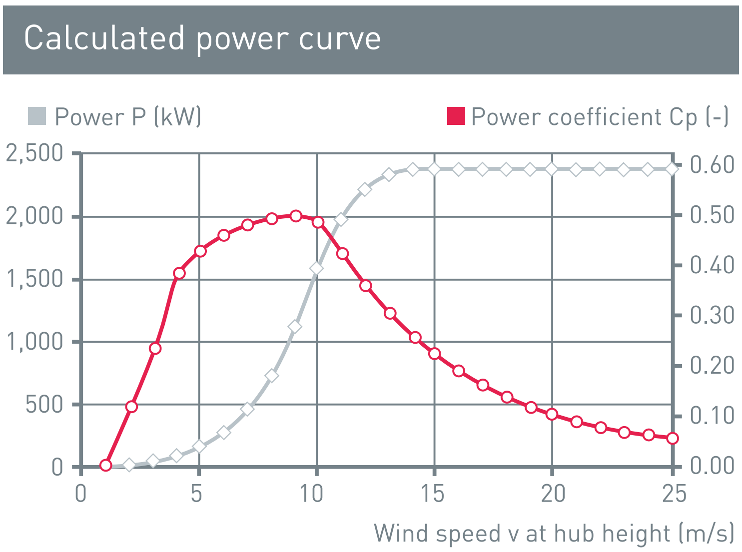

Figure A.2: *Power curve of the reference WT*

	E_{inv} [TWh]	EROI
Old program	42.1	8.78
New program	42.6	8.68

Table A.1: *Comparison of the objectives with the new approximations and corrections of errors*

A.1.2 Validation of the new program

As the program has been completely redesigned, the new program has to be validated in order to be sure that design and utilization changes did not affect the systems results. The only changes that should affect the results are the aforementioned "precisions" and "errors". Please find in Table A.1 the difference induced by the previously cited changes. Once these changes are reset to old approximations, the system, even with a different architecture, produces the exact same LP.

A.2 Use of the program

This section explains briefly how to use the program available in open source hosted on Github. Two files have to be understood to run the program.

main The main file centralizes the different aspects of the program. 4 important parameters to be chosen by the user appear clearly: simulationfile (represent the system one wants to launch, for example six cells), loglevel (which is a scalar from 0 to 2 which decides for the simulation to show few or more information during the simulation), loadresults (loads an already computed simulations to have instantly the results available, the results are stored in the "results" folder) and saveresults (stores the results of the computed simulation into a pickle file). Running the main.py file launches the simulation.

case The file "Case" is used to centralize all the information needed for the system chosen: timestep, use of TD, how much TD, amount of runs of the k - medoids (replicate) if the system does not load pre-calculated data.

Appendix B

Validation appendix

B.1 Choosing the number of typical days

In order to validate correctly the approximation of our data, a number of clusters has to be determined in function of our problem complexity. A thorough study of results in function of the number of clusters is conducted in section 3.2.1. This appendix will conduct a preliminary behaviour study solely on our clustering program. A balance between computation time and error has to be achieved in order to keep viable results in a reasonable amount of time. Comparing those two variables for a same system seems to clear an "elbow" (clear change in variation). This point characterizes a turning point where improving the problem complexity doesn't improve considerably the model's precision.

Considering the evolution of the error with the number of clusters in Figure B.1 for a one cell system (in this case, British Isles), a number of five TD seems a relevant balance for the following simulations. A second study has also been conducted in Figure B.1 on the two cells system (in this case, British Isles and Germany & Benelux). We can observe that, probably due to an increase in problem complexity, the position of our previously described "elbow" seems to be increasing to eight TD. This quantity is solely used for the two cells validation. Indeed, an increase in precision may be needed, even at the expense of computation time and problem complexity, if the tolerance on the system results is set at a different level. Please note that the error is quantified by the normalized euclidean distance, such as described in equation 2.1. The load duration curve of the advised 5 clusters can be found in Figure B.2.

B.2 Validation of one cell

As a fixed deviation criteria of 5 % was chosen to assess the approximation, one can see the correct approximation of 8 to 48 TD for the one cell system of British Isles. The divergence in results happens at 4 TD, moment where the time-series generated by the typical days is not sufficient to generate the approximation within the 5% deviation.

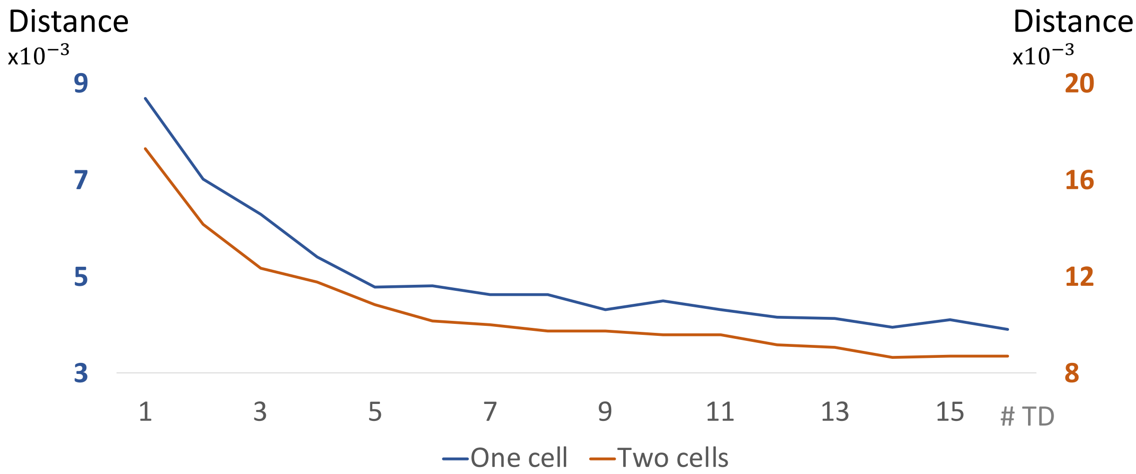

Figure B.1: *Variation between the number of cluster (TD) used and the precision of the clustering (expressed in normalized euclidean distance) for a one cell system and two cells system*

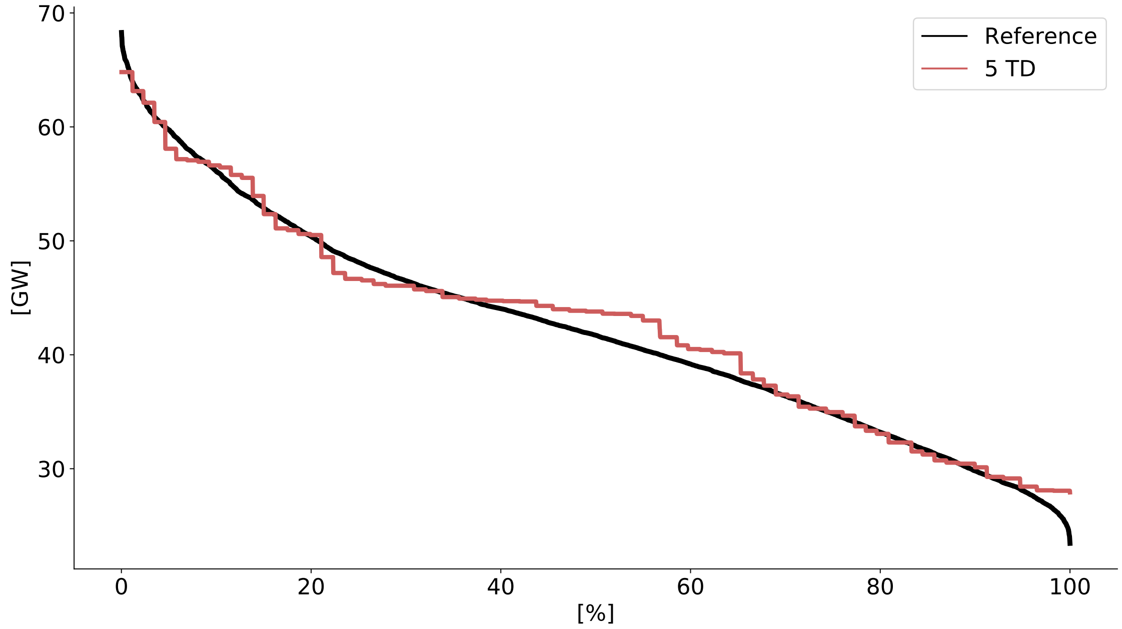

Figure B.2: *Load duration curve expressing the percentage of use of the power generation capacity for two models: reference model [34] and TD model with 5 clusters*

One cell **British Isles**	*Ref.*	*48 TD*	*24 TD*	*12 TD*	*8 TD*	*4 TD*	*Units*
PV	127	127	127	127	127	127	km^2
WT onshore	47603	45349	52534	50345	2956	29104	WT's
WT offshore	1277	1277	1277	1277	26563	7637	WT's
Batteries	722	589	227	265	420	505	GWh
Power-to-Gas	190	193	226	208	106	22	GWh
Gas storage	40	52	51	49	46	15	GWh
Curtailment	0	0	0	0	0	0	%
E_{inv}	45.1	42.9	46.6	44.9	49.9	38.3	TWh
EROI	8.2	8.7	7.8	8.1	7.1	8.8	/

Table B.1: *Results comparison of one cell (British Isles) between the reference model and the TD model with a variable number of clusters*

B.3 Validation of six cells and discussion

As the complexity of the system increased, so did the research of typical days. As one can note in Table B.2, the precision of the approximation of the TD decreased with the complexity of the system. Indeed, finding the TD were extremely tedious with the k - medoids method for the full 6 cells and the vast majority of the TD found were unfeasible problems. The 24 TD (1) in the table was found with the k-medoids by putting in a high amount of processing power. The other TD that did make up for the table were obtained thanks to Gauthier Limpens and the Dominguez method [24]. Even if the results are not into the 5% deviation criteria, the fact that these TD do not produce unfeasible problems show that this method produces more precise approximations. Given some computation time and processing power, correct TD could be found. As the TD from the Dominguez method were used, 16, 20, 28 and 34 TD produced unfeasible problems. The number of typical days of 42 and 46 produced coherent results but took a higher computation time than the reference scenario. For one wanting to simulate those TD, the simulation is stored in pickle files in the file "results" of the program cited previously , available on Github.

As the processing power needed to generate results for six cells in a time step of one meant a high computation time on a classical 2.4 *GHz* Intel Core i5, Adrien Couplet kindly allowed the use of his Intel Xeon CPU 3.2 *GHz*, 8 cores to reduce the computation time.

Six cells : NWE	*Ref.*	*38 TD*	*30 TD*	*24 TD(1)*	*24 TD(2)*	*Units*
British & Isles						
PV	127	127	127	127	127	km^2
WT onshore	45,834	51,448	58,864	41,885	52,952	WT's
WT offshore	1,277	1,277	1,277	1,277	1,277	WT's
Batteries	793	655	562	385	630	GWh
Power-to-Gas	178	210	243	179	224	GW
Gas storage	38	70	44	26	39	TWh
Curtailment	0	0	0	0	20	%
Germany & Benelux						
PV	3,750	3750	3,749	3,750	3,749	km^2
WT onshore	105,216	123,152	137,911	124,379	127,635	WT's
WT offshore	1,441	1,441	1,441	1,441	1,441	WT's
Batteries	3,821	3,906	5,433	2,198	4167	GWh
Power-to-Gas	181	149	200	174	224	GW
Gas storage	100	70	96	100	100	TWh
Curtailment	0.8	2.1	0.3	4.3	0.4	%
France						
PV	401	434	587	362	76	km^2
WT onshore	2,708	2,708	2,708	2,708	22,708	WT's
WT offshore	25,188	26,372	28,557	24,089	32,512	WT's
Batteries	3,620	1670	1,534	380	3,207	GWh
Power-to-Gas	51	84	92	90	96	GW
Gas storage	31	27	35	21	34	TWh
Curtailment	0	0	0	0	0	%
Scandinavia						
PV	7	7	7	7	7	km^2
WT onshore	6,571	2,412	2,412	2,412	4,133	WT's
WT offshore	2,764	5,666	6,525	6,571	5,667	WT's
Batteries	31	10	37	10	61	GWh
Power-to-Gas	2	0	1	9	2	GW
Gas storage	0.1	0	0	0.1	0	TWh
Curtailment	1.2	0.8	0.7	0.7	0.9	%
Iberian Peninsula						
PV	1,067	1,070	1300	788	1,177	km^2
WT onshore	16,974	17,311	16,106	20,167	16,522	WT's
WT offshore	1	1	1	1	1	WT's
Batteries	341	410	385	288	371	GWh
Power-to-Gas	73	54	57	86	74	GW
Gas storage	27	24	37	26	49	TWh
Curtailment	0	0	0	0	0	%
Italy & Alpine States						
PV	1,282	1,672	1,918	1,454	1,325	km^2
WT onshore	28,440	28,052	23,560	27,530	32,069	WT's
WT offshore	0	0	0	0	0	WT's
Batteries	428	476	557	294	406	GWh
Power-to-Gas	83	82	73	102	113	GW
Gas storage	39	47	52	39	69	TWh
Curtailment	0.7	0.1	0.1	1.3	0	%
E_{inv}	349	368	400.1	336.8	385.8	TWh
EROI	8.5	8.1	7.3	9	7.6	/

Table B.2: *Results comparison of two cells (British Isles and Germany & Benelux) between the reference model and the TD model with a variable number of clusters*

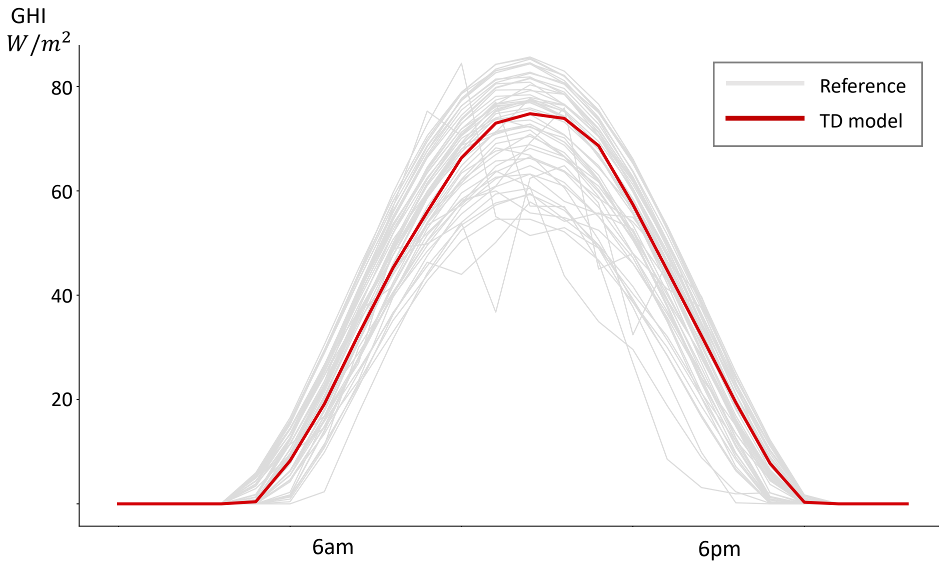

Figure B.3: *Expressing the GHI (Global Horizontal Irradiance) data of reference and 1 cluster in function of the time in the day*

B.4 Typicals days comparison for a same time-frame

As the method of TD tends to approximate the reference scenario, it has not the ambition to accurately approximate every hour of every day. Indeed, macro-metrics such as shares or total energies have to be compared in order to be relevant. This section shows some main trends for one and two cells between the reference method and the TD method.

One cell We can observe in Figure B.4 a comparison of a same time - frame for a same cell (British Isles, time step of one) between the two different methods. Two trends during the week can be observed: high RE production (begin and end of the week) and heavy reliance on storage for low production days (middle of the week). An exact match between the two models is not the purpose here, the model approximates a whole year on basis of the EROI and does not differentiate the production mix leading to this optimal factor. Macro - factors such as shares or gross total production are more relevant for a precise comparison. More on this matter is developed in section 3.2.6 .

Multiple cells The same parallel is made between two cells as it has been done for one cell. Once again, we can observe homogeneous trends without specific exact results matching hour per hour. The introduction of a new cell paved the way to power exchange. Indeed, one can observe in Figure B.5 that power exchange has become an important term in the power balance by relieving part of the storage production. For the sake of illustration, the highly interconnected cells (6 GW of interconnection) of Germany & Benelux and France has been chosen. Please note that power exchange when production is lower than consumption is import and the opposite situation is export (under and above the consumption line respectively).

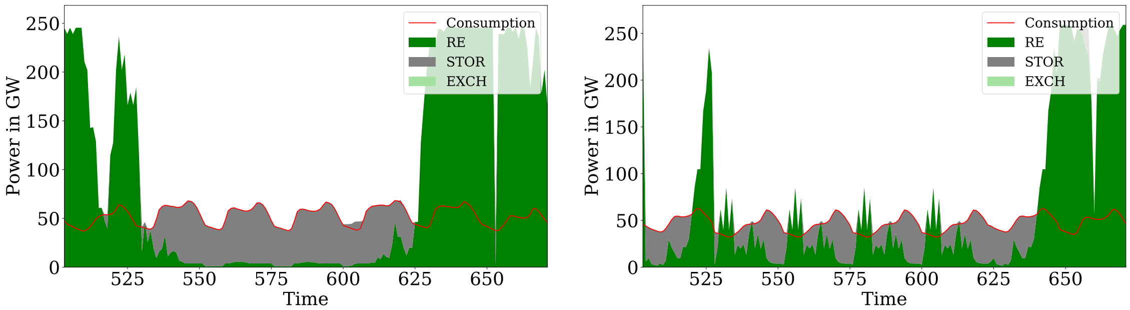

(a) *A week of power generation in the reference model*

(b) *A week of power generation in the TD model*

Figure B.4: *Comparison between the reference model and the TD model (12 clusters) for the same week in the British Isles*

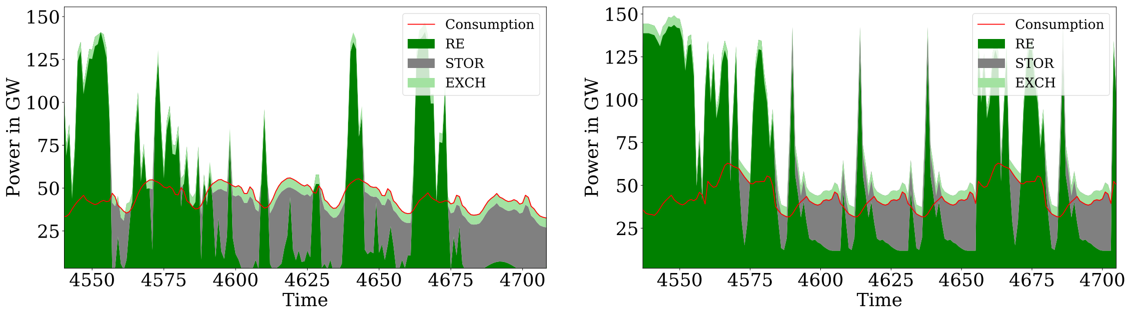

(a) *A week of power generation in the reference model*

(b) *A week of power generation in the TD model*

Figure B.5: *Comparison of France's cell between the reference model and the TD model (12 clusters) for the same week with power exchange from Germany & Benelux*

Appendix C

Results appendix

C.1 Full data of Commissions proposal

	Scand.	Brit. Isles	Ger. & Ben.	Fr.	It. & Alp.	Iber. Pen.
Gross Electricity	392 999	446 265	824 432	608391	480 082	335 296
Nuclear energy	49 738	107 051	4 047	385062	9 000	57 521
Solids	3 859	3 676	252 734	69	47 957	15 179
Oil (+refinery gas)	41	4 182	3 847	341	7 827	2 900
Gas (+derived gases)	17 489	113 489	216 677	12047	154 036	55 015
Biomass-waste	29 185	68 863	76 163	20256	29 616	11 878
Hydro	249 824	24 340	24 641	64139	134 301	52 372
Wind	42 019	110 982	175 701	83418	49 782	87 631
Solar	843	13 214	69 653	41048	41 339	52 590
Geothermal	0	466	969	2011	6 222	208

Table C.1: *Data used in the commission's proposal expressed in GWh*

C.2 EROI roadmap : energyflows

The monthly energy flows of Italy & Alpine states, Scandinavia and the British Iles can be found in Figure C.1, C.2, C.3 respectively. An energy flow diagram of the previous study on a 100% RE scenario is depicted in Figure C.4 for comparison.

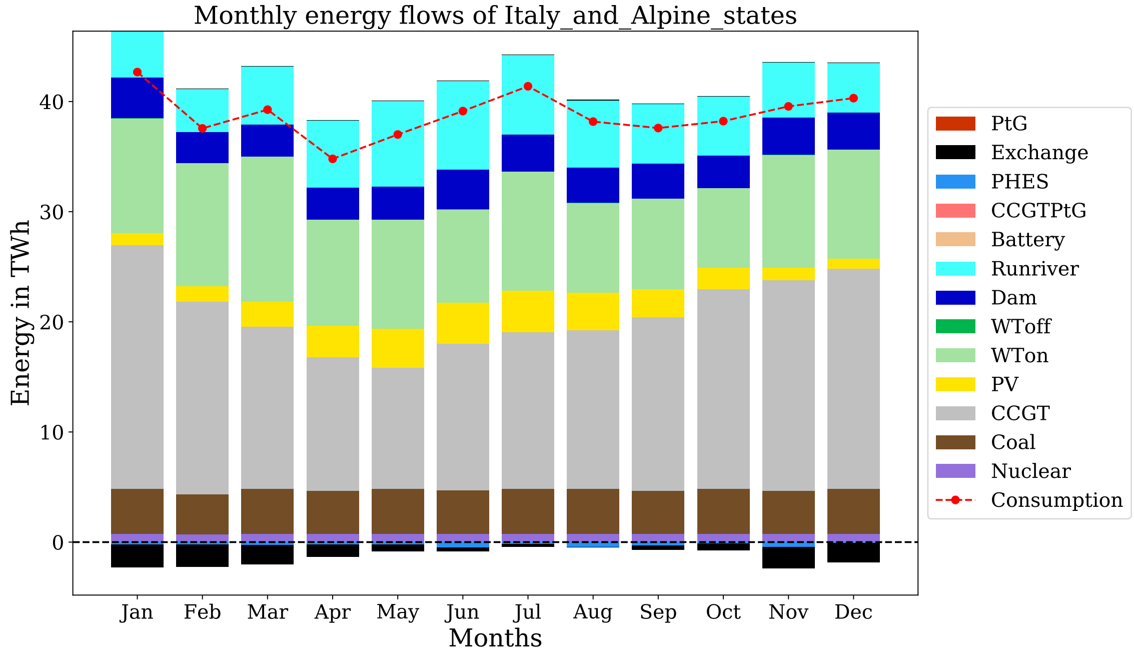

Figure C.1: *Monthly energy flows of the cell Italy& Alpine States in the EROI roadmap*

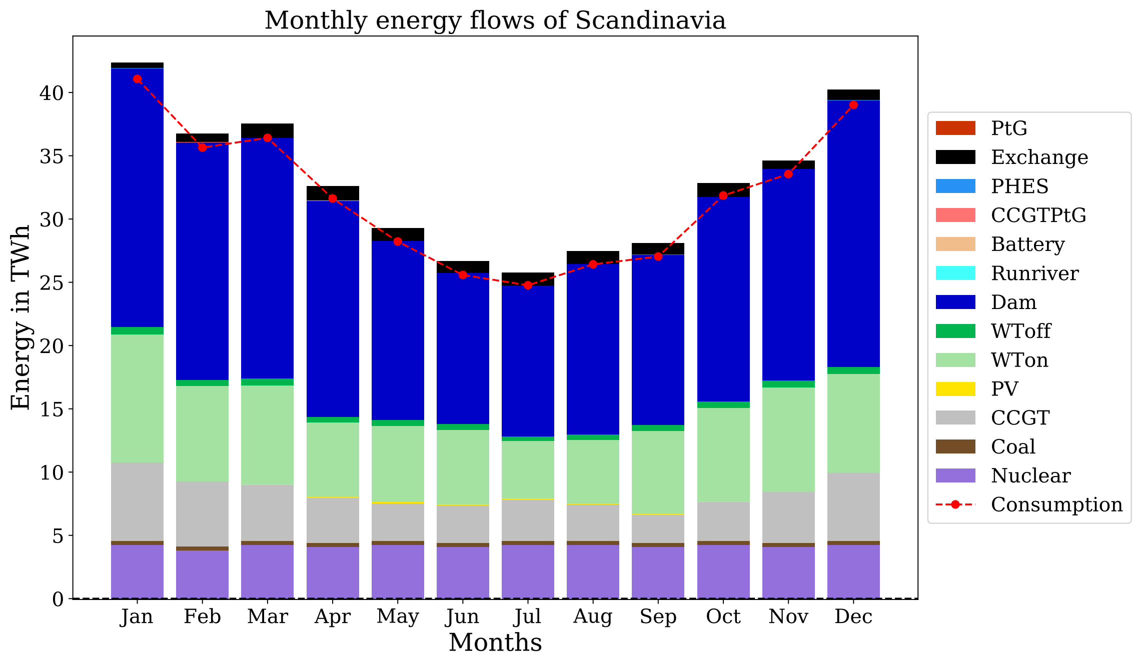

Figure C.2: *Monthly energy flows of the cell Scandinavia in the EROI roadmap*

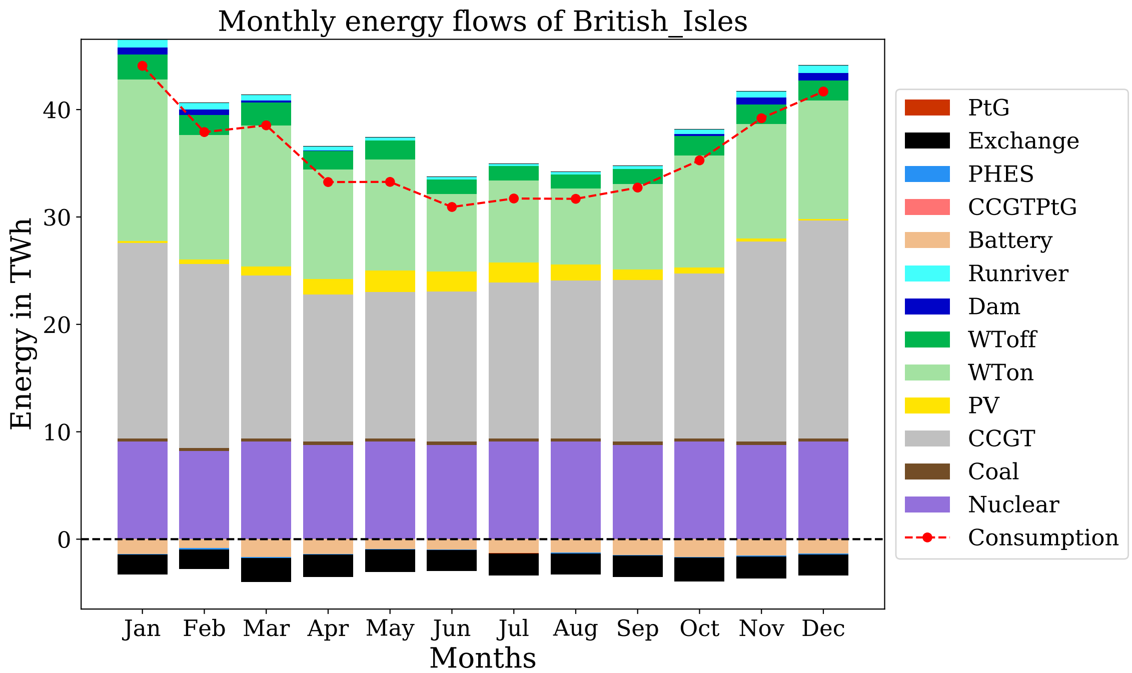

Figure C.3: *Monthly energy flows of the cell British Isles in the EROI roadmap*

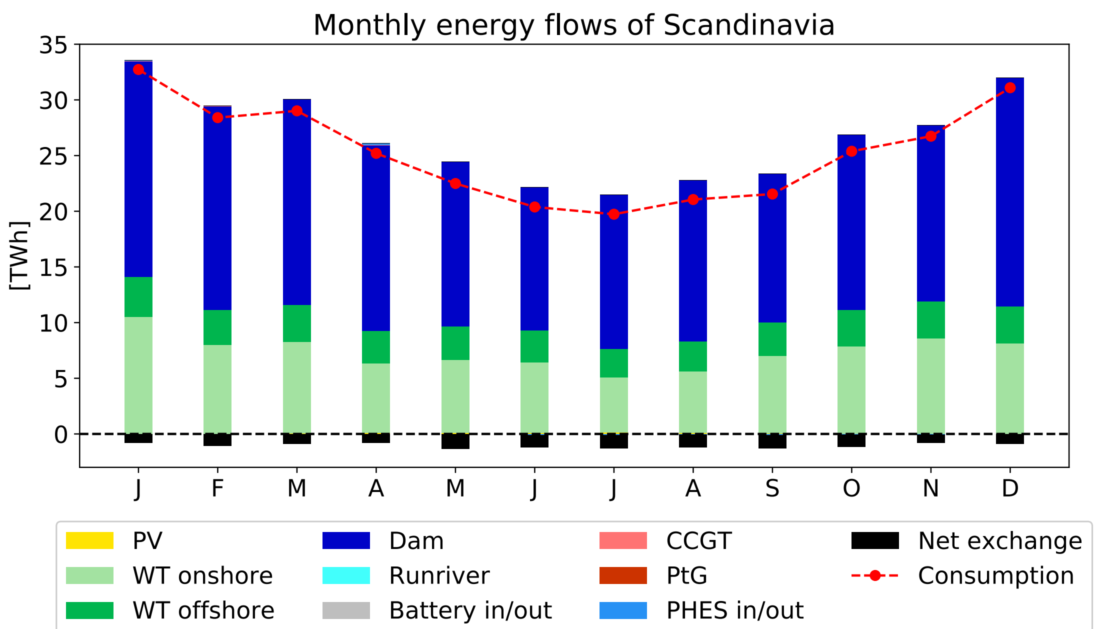

Figure C.4: *Energy flows of the scandinavian cell in a 100% RE scenario, adapted from [34]*

European wind The average European wind per region can be found in Figure C.5.

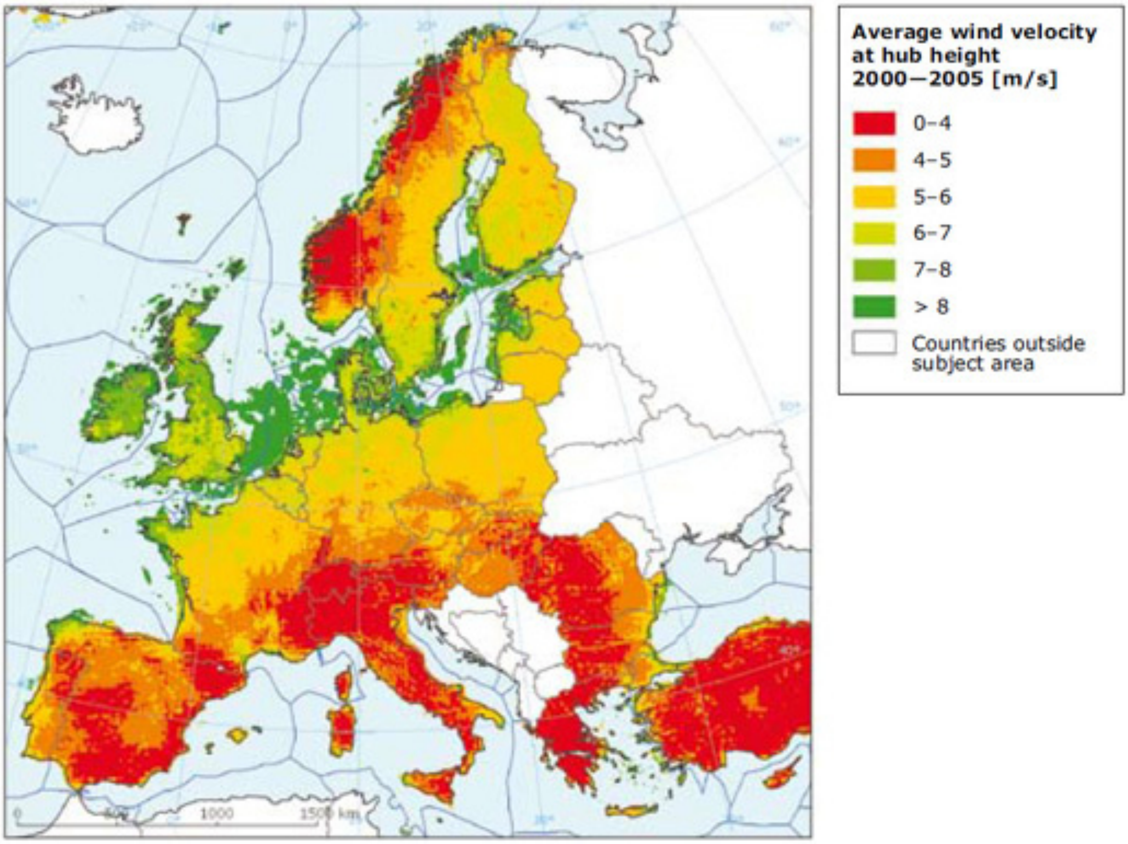

Source: EEA, 2008.

Figure C.5: *Wind velocity across NWE, from EEA 2008*

C.3 Details of emissions

Emissions	*1GWh*	Scandinavia	British Isles	Ger. & Ben.	France	It. & Alp.	Ib. Pen?
Coal	820	3,164	3,014	207,241	56	39,325	12,446
Gas	490	8,569	55,609	106,171	5,903	75,477	26,957
Nuclear	12	596	1,284	48	4,620	108	690
Biomass	230	6,712	15,838	17,517	4,658	6,811	2,732
Wind	11	462	1,220	1,932	917	547	963
PV	45	37	594	3,134	1,847	1,860	2,366
Total emissions		19,543	77,562	336,046	18,003	124,130	46,157
Mean g CO2/kWh		50	174	408	30	259	138
Actual g CO2/kWh		40	456	453	64	263	252

Table C.2: *Comparing the actual emissions per cell to that of the commission's proposal. Data from OECD.*

C.4 Relative importance of the RE of each cell

One can observe in the Figure C.6 multiple behaviours. Scandinavia has very quickly a high share of the system's RE which decreases then relatively to the other cells dominance. The cell Italy & Alpine States seems to have on another hand a steady increase in renewables, possessing thus a nearly constant relative share in the mix. On the other hand, Germany & Benelux seems to have a steady share throughout the scenarios until a 100 % renewables share is imposed, moment where the cell takes on the biggest RE production of the system. The British Isles tend to a 100% cell from scenario 50% up to 80 % with thus an increasing relative RE share.

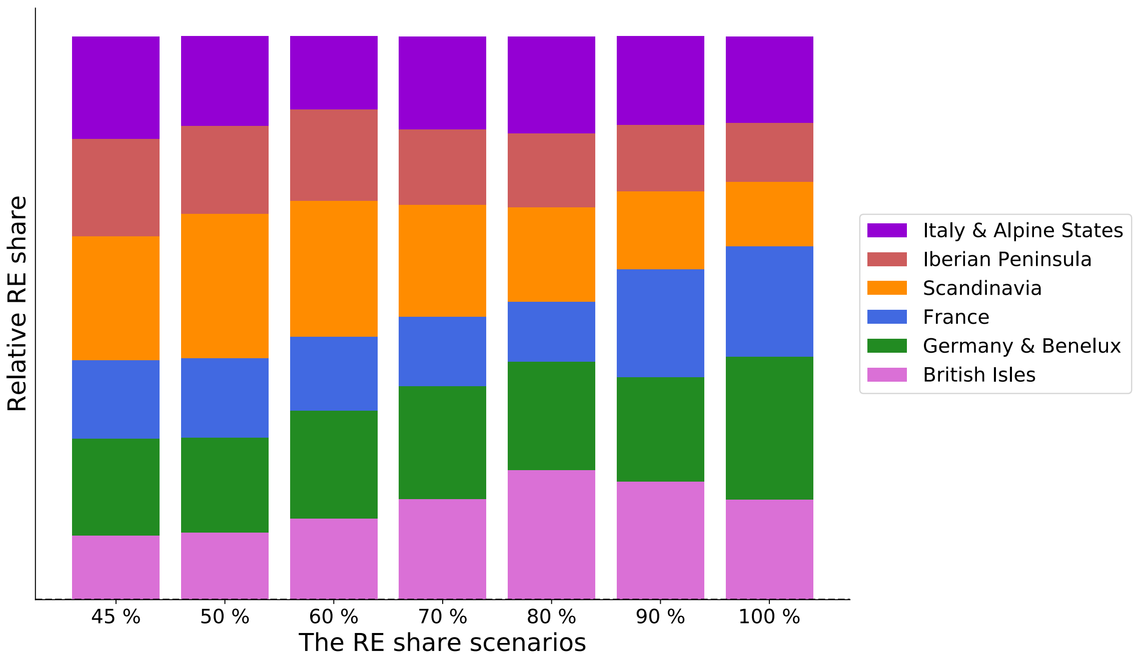

Figure C.6: *Evolution of the relative importance of RE of each cell to the different RE constraints on the whole NWE system*

Bibliography

[1] Effects of north-african electricity import on the european and the italian power systems: a techno-economic analysis. *Electric Power Systems Research*, 96:119 – 132, 2013.

[2] W. Zappa W. C. Turkenburg A. S. Brouwer, M. van den Broek and A. Faaij. Least-cost options for integrating intermittent renewables in low-carbon powersystem. *Elsevier, Applied Energy*, 2016.

[3] Danish Energy Agency. The danish energy model: Innovative, efficient and sustainable, 2018.

[4] Danish Energy Agency. Denmark's energy and climate outlook 2018 baseline scenario projection towards 2030 with existing measures (frozen policy), 2018.

[5] International Energy Agency. Status of power system transformation 2019. Paris, France, 2019.

[6] Head of International Energy Affairs Ambassador Jean-Christophe Fueeg. Switzerland energy strategy 2050, 2016.

[7] Markus Biberacher. Modelling and optimisation of future energy systems using spatial and temporal methods. 2007.

[8] Matthew J. Burke and Jennie C. Stephens. Political power and renewable energy futures: A critical review. *Energy Research and Social Science*, 35:78 – 93, 2018. Energy and the Future.

[9] S. Hilpert C. Wingenbach C. Kaldemeyer, M. Sothe. renpassg!s - a free andopen python tool for simulating energy supply systems. *OSF*, 2016.

[10] C. Cany, C. Mansilla, G. Mathonnière, and P. da Costa. Nuclear power supply: Going against the misconceptions. evidence of nuclear flexibility from the french experience. *Energy*, 151:289 – 296, 2018.

[11] European Commission. Communication from the commission to the european parliament, the council, the european economic and social committee and the committee of the regions, 2011.

[12] European Commission. Energy roadmap 2050: Impact assessment and scenario analysis, 2011.

[13] European Commission. Eu reference scenario: Energy, transport and ghg emissions trends to 2050, 2016.

[14] European Commission. A clean planet for all: a european long-term strategic vision for a prosperous, modern, competitive and climate neutral economy, 2018.

[15] European Commission and International Renewable Energy Agency. Renewable energy prospects for the european union, 2018.

[16] David Connolly and Brian Vad Mathiesen. A technical and economic analysis of one potential pathway to a 100renewable energy system. *International Journal of Sustainable Energy Planning and Management 1*, 2014.

[17] R.K. Pachauri Core Writing Team and L.A. Meyer (eds.). Climate change 2014: Synthesis report. contribution of working groups i, ii and iii to the fifth assessment report of the intergovernmental panel on climate change. 2014.

[18] Deger Saygin (IRENA) Dolf Gielen (IRENA) and Nicholas Wagner (IRENA). Renewable energy prospects: Germany, remap 2030 analysis. *IRENA*, pages 54 – 56, 2015.

[19] Anne Sjoerd Brouwer et al. Least-cost options for integrating intermittent renewables in low-carbon power systems. *Applied Energy 161*, 2016.

[20] Fernando Dominguez-Munoz et al. Selection of typical demand days for chp optimization. *Energy and Buildings*, 43(11):3036 – 3043, 2011.

[21] Kari Aamodt Espegren Eva Rosenberg. Future energy demand - a norwegian overview. *Institute for Energy technology*, 2013.

[22] Federal Ministry for Economics Affairs and Energy. Fifth "energy transition" monitoring report: the energy of the future, 2015.

[23] Hervé Jeanmart Gauthier Limpens. Electricity storage needs for the energy transition: An eroi based analysis illustrated by the case of belgium. *Elsevier, Energy*, 2018.

[24] Hervé Jeanmart Gauthier Limpens, Stefano Moret and Francois Marécha2. Energyscope td: an open source model for national energy systems. *Institute of Mechanics, Materials and Civil Engineering, Université catholique de Louvain, Belgium*, 2019.

[25] B. Jansen, J.J. de Jong, C. Roos, and T. Terlaky. Sensitivity analysis in linear programming: just be careful! *European Journal of Operational Research*, 101(1):15 – 28, 1997.

[26] S. Lloyd. Multivariate cointegration and causality between exports, electricity consumption and real income per capita: Recent evidence from japan. *International Journal of Energy Economics and Policy*, 1(3):59–68, 2011.

[27] N. Strachan C. Heaps H. Huntington S. Kypreos A. Hughes S. Silveira J. DeCarolis M. Bazillian A. Roehrl M. Howells, H. Rogner. Osemosys: the open-source energy modeling system: an introduction to its ethos, structure anddevelopment. *Energy Pol. 39*, 2011.

[28] Ioannis P. Panapakidis and Georgios C. Christoforidis. Optimal selection of clustering algorithm via multi-criteria decision analysis (mcda) for load profiling applications. *Applied Sciences*, 8(2), 2018.

[29] Ioannis P. Panapakidis and Georgios C. Christoforidis. Optimal selection of clustering algorithm via multi-criteria decision analysis (mcda) for load profiling applications. *Applied Sciences*, 8(2), 2018.

[30] Emanuele Martelli Marco Mazzotti Paolo Gabrielli, Matteo Gazzani. Optimal design of multi-energy systems with seasonal storage. *Elsevier, Applied Energy*, 2017.

[31] Stefan Pfenninger, Lion Hirth, Ingmar Schlecht, Eva Schmid, Frauke Wiese, Tom Brown, Chris Davis, Matthew Gidden, Heidi Heinrichs, Clara Heuberger, Simon Hilpert, Uwe Krien, Carsten Matke, Arjuna Nebel, Robbie Morrison, Berit Müller, Guido Pleßmann, Matthias Reeg, Jörn C. Richstein, Abhishek Shivakumar, Iain Staffell, Tim Tröndle, and Clemens Wingenbach. Opening the black box of energy modelling: Strategies and lessons learned. *Energy Strategy Reviews*, 19:63 – 71, 2018.

[32] Marcelo Poppe and Lionel Cauret. Chapter vii - the french electricity regime. In Atle Midttun, editor, *European Electricity Systems in Transition*, Elsevier Global Energy Policy and Economics Series, pages 199 – 229. Elsevier Science Ltd, Oxford, 1997.

[33] Erich Schubert and Peter J. Rousseeuw. Faster k-medoids clustering: Improving the pam, clara, and CLARANS algorithms. *CoRR*, abs/1810.05691, 2018.

[34] Sylvain Ramelot Thibault Martinelle. Study of a 100% renewable electricity system for western europe: an eroi-based analysis. *Université Catholique de Louvain, Belgium*, 2018.

[35] Vicente Valle Jr. Chaos, complexity and deterrence. *National Defense University National War College Washington, DC*, 19 Apr 2000.

[36] Hans Christian Gils Yvonne Scholz and Robert C Pietzcker. Application of a high-detail energy system model to derive power sector characteristics at high wind and solar shares. *Energy Economics 64*, 2017.

[37] Computer Engineering Department Üniversiteler Mahallesi, Middle East Technical University. *K-Means Clustering Demo*, 2018.

UNIVERSITÉ CATHOLIQUE DE LOUVAIN
École polytechnique de Louvain
Rue Archimède, 1 bte L6.11.01, 1348 Louvain-la-Neuve, Belgique | **www.uclouvain.be/epl**